Paleobiology, 33(4), 2007, pp. 610–638

Craniocervical feeding dynamics of *Tyrannosaurus rex*

Eric Snively and Anthony P. Russell

Abstract.—*Tyrannosaurus rex* and other tyrannosaurid theropods exerted high bite forces, and large muscle attachments suggest that the tyrannosaurid neck was a concomitantly powerful component of the feeding apparatus. We examine accelerative and work-generating capacity (WGC) of neck muscles in adult *Tyrannosaurus rex*, using a 3-D vector-based method that incorporates aspects of muscle force generation, reconstruction of muscle morphology and moment arms, and rotational inertias of the head and neck. Under conservative assumptions, radial accelerations of the head by large superficial muscles (M. transversospinalis capitis, M. complexus, and M. longissimus capitis superficialis) enabled rapid gaze shifts and imparted high tangential velocities to food sufficient for inertial feeding. High WGC by these and deeper muscles under eccentric contraction indicate high efficacy for tearing flesh, especially with the head and neck in an extended posture. Sensitivity analyses suggest that assigned density of the antorbital region has substantial effects on calculated rotational inertia, and hence on the accuracy of results. However, even with high latitude for estimation errors, the results indicate that adult *T. rex* could strike rapidly at prey and engage in complexly modulated inertial feeding, as seen in extant archosaurs.

Eric Snively and Anthony P. Russell. Department of Biological Sciences, University of Calgary, 2500 University Drive NW, Calgary, Alberta T2N 1N4, Canada. E-mail: esnively@ucalgary.ca, arussell@ucalgary.ca*

*Present address: *Department of Biological Sciences, CW405 Biological Sciences Centre, University of Alberta, Edmonton, Alberta T6G 2E9, Canada*

Accepted: 26 April 2007

Introduction

Tyrannosaurid dinosaurs, from the Campanian and Maastrichtian of Asia and North America, were the largest macropredaceous coelurosaurs (Holtz 2004). Tyrannosaurids differed adaptively from other large theropods (500–10,000 kg) in appendicular and feeding specializations. Gracile hind-limb proportions and an arctometatarsus enhanced speed and agility in tyrannosaurids (Coombs 1978; Holtz 1994, 1995; Snively and Russell 2002, 2003; Snively et al. 2004), while the relatively small forelimbs retained only two functional digits. Adult tyrannosaurids lacked the relatively elongate skulls seen in giant carcharodontosaurid carnosaurs, and instead had broad crania, fused nasals, a deep lower jaw, and otherwise reinforced head skeleton (Henderson 2002; Holtz 2002; Rayfield 2004, 2005; Therrien et al. 2005; Snively et al. 2006) that delivered adductor forces capable of breaking the bones of prey (Molnar 1973; Erickson et al. 1996; Meers 2003; Wegweiser et al. 2004).

Jaw function of tyrannosaurids and other theropods has been well characterized (Molnar 1973, 1998 [2000]; Erickson et al. 1996; Rayfield 2004, 2005; Therrien et al. 2005), but the role of the neck in feeding has remained largely unstudied, aside from perceptive observations of Bakker et al. (1988), Paul (1988), Bakker (1998 [2000]), and Rayfield et al. (2001). In contrast with other large theropods that could use longer, powerful forelimbs for subduing prey (Charig and Milner 1997; Senter and Robins 2005), the neck and jaws of many tyrannosaurids were probably the sole mechanism of prey apprehension. Tyrannosaurids had relatively larger insertions for some neck muscles than did other large theropods (Paul 1988). We explore the contribution of tyrannosaurid neck muscles to feeding by reconstructing their capacity to produce torque and perform work in an exemplar specimen, an adult *Tyrannosaurus rex*.

The ability of muscles to do work involves resisting and overcoming loads involved in feeding and other activities. We term a muscle's potential performance to exert a force over a distance its ''work-generating capacity'' (WGC), which combines its moment-generating capacity with the expected loads a

 0094-8373/07/3304-0007/$1.00

muscle encounters during activation. The rotational and translational inertias of these loads must be factored into the muscle's WGC; muscles that can generate high torque may be able to perform little work if the loads are too high. This might be the case for an amniote with a very large head or weak neck, which must expend muscular energy to maintain head posture and have little in reserve for moving the head and/or acquiring food. An amniote with a large head but a powerful neck, however, will have a higher WGC and more capability to maneuver the feeding apparatus. WGC therefore describes a muscle's capabilities above the minimum required for postural maintenance.

The potential capacity to perform work does not mean that the work is always positive; a muscle with a high WGC will exert high torque but perform no work under isometric contraction, and experience negative work under eccentric contraction when the muscle is lengthening. However, WGC provides a good indication of a muscle's contribution to feeding performance.

The quantitative index of WGC used here is the actual or theoretical angular acceleration that a muscle could impart to a body segment, if it were undergoing concentric contraction at concentric, isometric, or eccentric levels of force. The muscle cannot perform positive work when contracting isometrically or eccentrically. Instead, the theoretical accelerations at these levels of force indicate the capacity of muscles in *Tyrannosaurus rex* to perform work involved in tearing prey tissues, when the head is held steady or the neck is being stretched. Force and work-generating capacity at these levels are based on performance parameters involved in force production in extant animals, and hypotheses of feeding in *T. rex* are based on observations of feeding behavior in extant archosaurs.

Goals and Hypotheses

Analysis of feeding in predatory birds (Snively 2006) suggests capabilities of biological importance to a feeding *Tyrannosaurus rex*. These include the ability to lift the head away from the food and look from side to side to assess the surroundings, as after attack or swallowing food. Raptors often tear flesh by rearing back with their hind limbs, and their necks must withstand high, externally imposed loadings. The capability to withstand analogous sagittal loadings, and those imposed by lateral flexion when tearing flesh, are testable for *T. rex*. After excising flesh or when eating larger prey, raptors engage in inertial feeding similar to that seen in other reptiles. If *T. rex* analogously tossed large bodies of food back in the throat, it would have had to accelerate its head vertically to overcome the inertia of the food, and of its own head and neck. We therefore use results of musculoskeletal dynamic calculations to estimate four performance magnitudes and test three hypotheses related to *T. rex* feeding.

Magnitude 1: Maximum vertical acceleration of the head with the feeding apparatus passing through a neutral posture.

Magnitude 2. Maximum vertical load with the feeding apparatus passing through a neutral posture, as the muscles were being stretched by the load.

Magnitude 3: Maximum lateral acceleration of the head with feeding apparatus passing through a neutral posture.

Magnitude 4. Maximum lateral load with the feeding apparatus passing through a neutral posture, as the muscles were being stretched by the load.

Hypothesis 1: Moment-generating capacity of head dorsiflexors increased as the head was dorsiflexed.

Hypothesis 2: Moment-generating capacity of head lateroflexors increased from the point of maximum left lateral flexion to the neutral posture, and decreased as the head continued to be swept to the right.

Hypothesis 3: The mouth of the examined specimen of *Tyrannosaurus rex* appears capable of encompassing approximately 50 liters, and therefore 50 kg, of food with an average specific gravity of 1. We test the hypothesis that the craniocervical muscles could impart sufficient acceleration to the head, neck, and a 50 kg bolus of food (with its center of mass medial to the large anterior maxillary teeth), to conduct inertial feeding.

Hypotheses 1 and 2 describe possible scenarios of head motion in *T. rex* when the ani-

mal shifted its gaze, or struck laterally at prey by lateroflexion or anteriorly by dorsiflexion. They derive from the observations that muscle moment arms appear to have been most favorable in the neutral posture, and thus accelerations of the head are predicted to have been greatest when the head moved through this position.

Because many parameters of musculoskeletal function in fossil animals must be inferred or estimated, sensitivity analyses are highly instructive about the effects of uncertainty of assigned values (Hutchinson and Garcia 2002; Hutchinson 2004a,b). Origins and insertions of major neck muscles are well characterized for *T. rex* (Snively 2006), and deviations from the animal's true morphology entail predictably linear errors, or cosine errors that will be small (Richmond 1998), even with ostensibly gross mischaracterization of muscle attachment topology. Variabilities of other parameters would have nonlinear and complex combinatorial effects, and are potentially greater sources of error.

We conducted three sensitivity analyses to test the effects of variability and error in various musculoskeletal parameters on inference of inertial feeding in *T. rex* (hypothesis 3):

1. Sensitivity of accelerations to the presence or absence of interspinous ligaments. Accelerations are calculated with and without inferred ligamentous support against gravity.
2. Effects of head density and inertial properties on accelerations. Different assigned densities of the antorbital region test the sensitivity of dorsiflexive accelerations to inertial properties of the head.
3. Sensitivity of sagittal accelerations to errors of moment estimation, and to muscle recruitment patterns. Moment-generating capacities of head dorsiflexors, contracting unilaterally and bilaterally, are tested for the ability to accelerate 490 N of food tangentially at 1.5 *g* (a sufficient value for inertial feeding).

Sensitivity analysis 3 yields indices of muscle recruitment latitude for a *T. rex* to be able to engage in inertial feeding with food of greater weight, and to reorient food in its mouth for swallowing, as seen in crocodilians. If a muscle easily imparts the minimum vertical velocity to the food for inertial feeding, more intense recruitment of this muscle, and additive recruitment of others, will be available for feeding on larger masses of food. High recruitment latitude for sagittal acceleration would impart (nearly literal) modulatory ''wiggle room,'' enabling the animal to accelerate the food in non-sagittal directions to reorient it in the mouth. Conversely, if a muscle is incapable of accelerating the food at a sufficient rate, its force must be augmented by recruitment of additional muscles. Accelerative capacity below the threshold necessary for inertial feeding compromises a muscle's autonomous utility for this biological role.

Morphological and Physiological Background for Tyrannosaurid Neck Dynamics

Neck Muscles of Tyrannosaurids

Tyrannosaurid neck muscles are described in greater detail elsewhere (Snively 2006). Table 1 lists origins and insertions of major muscles (spanning more than two vertebrae) in tyrannosaurids, with abbreviations given for all listed muscles. Bracketed (Witmer 1995) and extrapolatory reconstruction (Bryant and Russell 1992) indicates that tyrannosaurids had neck muscles variably similar to those of birds and crocodilians (Table 1, Fig. 1A) (Snively 2006). For example, anteriorly originating head dorsiflexive muscles of the M. transversospinalis group (Tsuihiji 2005), M. complexus and M. splenius capitis (hereafter abbreviated as M. spl. cap.), strongly resembled those of birds. The neck dorsiflexor M. transversospinalis cervicis (M. trans. cerv.) had large, crocodilian-like origins from the neural spines, but remarkably avian-like insertions on the epipophyses (Table 1). Despite the avian-like curvature of the tyrannosaurid neck, the largest head dorsiflexor, M. transversospinalis capitis (M. trans. cap.), had crocodilian-like origins from the tips of the neural spines. Its insertion on the parietals is relatively larger and more rugose than in crocodilians, suggesting a large muscle belly. The large lateroflexor M. longissimus capitis su-

TABLE 1. Origins and insertions of major neck muscles of *Tyrannosaurus rex*. Abbreviations are used throughout the text.

Muscle	Origin	Insertion
M. transversospinalis capitis = M. trans, cap.	Dorsal portion of neural spines	Rugose posterodorsal scar on parietal
M. complexus	C2–C5 epipophyses	Posterior surface of squamosal
M. splenius capitis = M. spl. cap.	Teardrop-shaped scar on C2	Posteroventral parietal fossa
M. transversospinalis cervicis = M. trans, cerv.	Lateral surface of neural spines	Epipophyses, especially onto concave C2 scar
M. longissimus capitis superficialis = M. long. cap. sup.	T1–C6 transverse processes	Lateral scar on exoccipital
M. longissimus capitis profundus = M. long. cap. prof.	C5–C2(?) transverse processes	Concave basituberal scar on basicoccipital
M. iliocostalis capitis = M. il. cap.	Proximal cervical ribs, rib fascia(?)	Ventral edge of exoccipital
M. rectus capitis ventralis = M. r. c. v.	Anterior cervical hypopophyses	Ventrally onto basitubera of basioccipital

perficialis (M. long. cap. sup.) originated from transverse processes and inserted onto the paroccipital processes, similarly to the attachments in non-avian amniotes (Rosse and Gaddum-Rosse 1997; Cleuren and De Vree 2000; Snively 2006). The work-generating capacity of all of these muscles was contingent on their dimensions, moment arms, and physiological properties.

Muscle Performance Variables in Extant Animals

A muscle's ability to produce force, work, and power depends on its contractile capabilities. Vertebrate skeletal muscle has similar physiology and contractile properties across taxa. Variations in fiber type composition, internal geometry of muscle fibers, muscle cross-sectional area, and length govern differences in the contraction of different muscles. The force that a muscle produces varies predictably with its length and velocity of contraction, with force generally increasing with length to a point, and decreasing with velocity. The muscle's fiber type composition and operating temperature influence contraction velocity, with the highest velocities from glycolytic, fast-twitch but rapidly fatiguing fibers, and relatively high but thermoneutral body temperatures. Dozens of dissected extant archosaurs have a preponderance of ''dark meat'' in their superficial neck muscles (especially in large birds; Snively 2006), suggesting that the muscles have predominately fast oxidative gycolytic fibers (Syme 2006) that can contract rapidly but recover quickly from fatigue. It is reasonable to assume the same properties in the neck muscles of tyrannosaurids, which fall within the phylogenetic bracket of birds and crocodilians (Witmer 1995). Adult *T. rex* was likely homeothermic with a body temperature of 35–40°C (Gillooly et al. 2006) favorable for muscle function. We assume that it experienced invariance of temperature influences on muscle force, contraction velocity, and power at given muscle lengths (Guyton and Hall 1996), and that its muscle physiological parameters were comparable to those of extant homeotherms.

Although different muscles will have similar force-velocity and force-length relationships (Syme 2006), the inherent force-generating capacity of an individual muscle is proportional to the number of sarcomeres in parallel. Hence, the force depends on the collective cross-sectional area of the muscle fibers (large in human power lifters [Akima et al. 2000; Brechue and Abe 2002]). The contraction force will equal this cross-sectional area times the muscle's specific tension, or the force it produces per unit area (Kawakami et al. 1995; Fukunaga et al. 2001).

Muscle Cross-sectional Area.—The summed physiological cross-sectional area (PCSA;

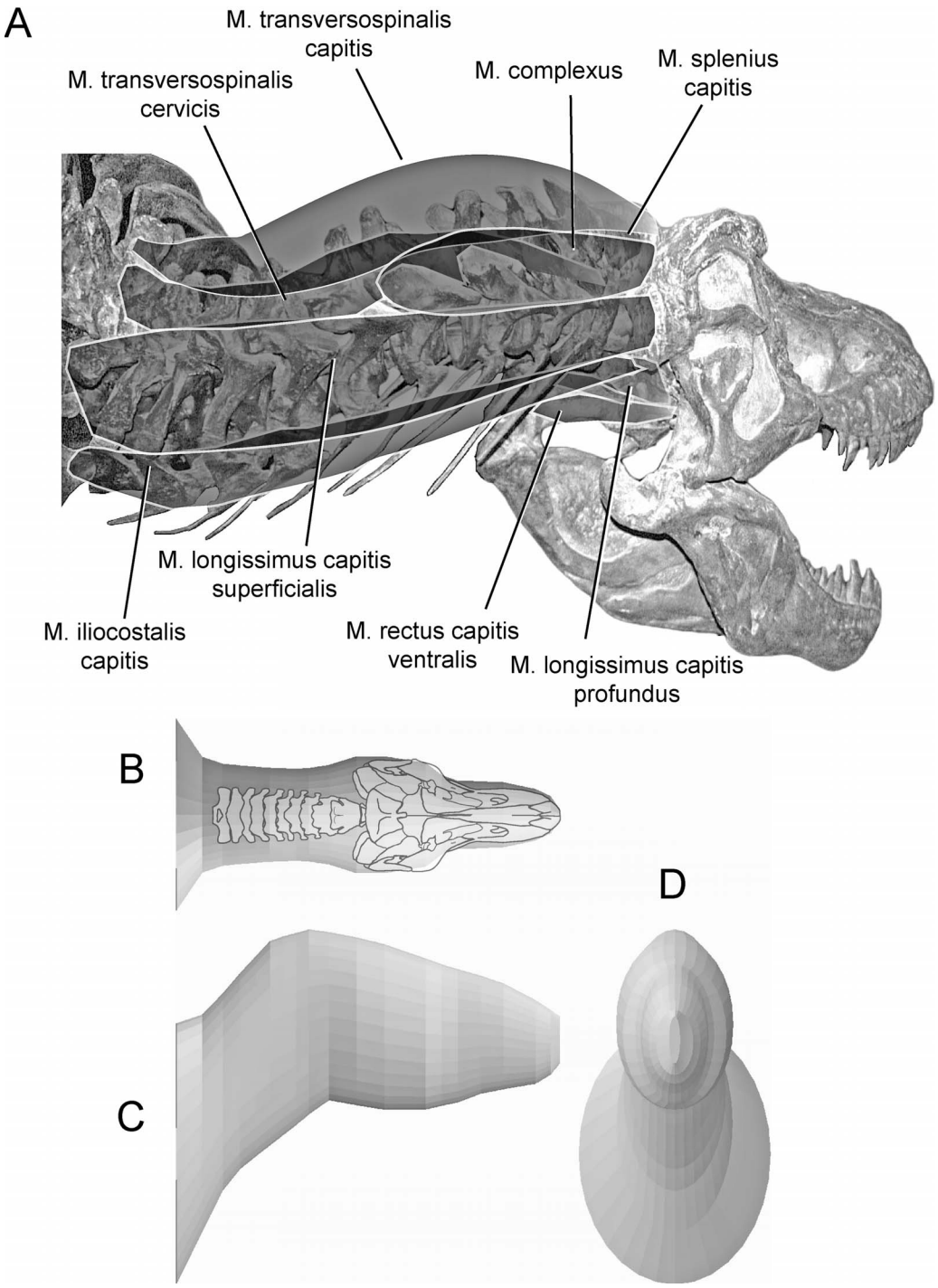

FIGURE 1. Anatomical and inertial reconstructions used for calculating neck dynamics of *Tyrannosaurus rex*. A, Superficially visible neck muscles mapped onto a skeleton of *Tyrannosaurus rex* AMNH 5027 (BMR cast), with the head and neck lateroflexed to the left. Insertions of M. transversospinalis cervicis onto anterior epipophyses are posteroventral to the origins of M. complexus from the same structures. B–D, 3-D computer representation of *Tyrannosaurus rex* (AMNH 5027) used to calculate gravitational moments and rotational inertias, in dorsal (B), lateral (C), and anterior (D) views. The skeleton is superimposed on the model in B; congruence is not absolute because the 3-D models are rendered in strict orthogonal view and the skeleton in perspective view.

Thorpe et al. 1999) of a muscle's fibers is often greater than the anatomical cross-section of a muscle, if the muscle is pennate with fibers angled relative to the line of muscle pull. In fusiform muscles, such as those involved in plantar flexion in humans (Bamman et al. 2000), PCSA is very close to anatomical cross-sectional area (ACSA). However, in highly pennate muscles, PCSA and force generation can be dramatically higher than would be estimated using anatomical cross-sectional area (Cheng and Scott 2000).

Physiological cross-sectional area (Richmond 1998; Vasavada et al. 1998) depends on a muscle's mass, m, volume and density (ρ, typically 1.06 $g \cdot cm^{-3}$), pennation angle (σ), and average (''optimal'') fascicle length (l, determined through dissection or magnetic resonance imaging [MRI: Juul-Kristensen et al. 2000; Akima et al. 2000]). When these quantities are known or estimated, PCSA can be calculated using the following equation:

$$\text{PCSA} = m \cdot \cos \sigma / l \cdot \rho. \quad (1)$$

Specific Tension.—Specific tension, ST, can be considered a stress, or force/area that a muscle produces. ST is fairly uniform in vertebrate muscle that is actively shortening by concentric contraction. In cat neck muscles ST is 24 $N \cdot cm^{-2}$ (Keshner et al. 1997), and in fusiform bellies of human leg muscles, in vivo ST is about 20-22 $N \cdot cm^{-2}$ (Bamman et al. 2000). Isometric ST, when a muscle is acting against resistance but not shortening, is approximately 30 $N \cdot cm^{-2}$ (Johnston 1985). Less often considered is the ST of a muscle when lengthening under a load, producing force by eccentric contraction. Maximum eccentric force of a muscle can exceed twice that attained during concentric contraction (Horstmann et al. 2001; Lindstedt et al. 2001).

A muscle's contractile force F_m is the product of PCSA and ST:

$$F_m = \text{PCSA} \cdot \text{ST}. \quad (2)$$

The quantities involved in calculating PCSA and ST have varying magnitudes of effect on muscle force. For example, pennation angle must exceed 25° (a rare occurrence) for force in a tendon's line of pull to be perturbed by more than 10% (Richmond 1998). Whereas force/sarcomere along the tendon's line of pull will diminish, the number of sarcomeres in parallel, and hence the muscle's physiological cross-sectional area, can increase substantially.

Most of these factors are impossible to assess directly for extinct taxa. However, most neck muscles in crocodilians and birds, the extant bracket of Mesozoic dinosaurs (Witmer 1995), appear to be fusiform. Their physiological cross-sectional areas are probably close to the estimated anatomical cross-sectional areas (ACSA).

Dynamic Modeling of Musculoskeletal Function

With equation (2) we can estimate the force a muscle produces, but its function in moving the skeleton will depend on its moment arm from the muscle's insertion to the point of joint rotation. The force component of the muscle perpendicular to the moment arm exerts a moment or torque, which acts to rotate the relatively mobile skeletal element about the joint.

There are two major approaches to calculating musculoskeletal torques, accelerations, and displacements—using either Newton-Euler free body diagrams (Hildebrand and Goslow 2001) or the partial velocity method (Yamaguchi 2001). Both methods incorporate masses and rotational inertias of body segments. The partial velocity method is strongly vector based, which simplifies treatment of motion in three dimensions. It has the advantage of specifying origins and insertions relative to a global reference frame, while treating each joint as involving rotation and translation in a local reference frame fixed on the immobile element. To explore *T. rex* neck dynamics, we use an algorithm that incorporates vectors and inertia similarly to the partial velocity method. Vectorized approaches have been validated in investigations of extant animals, including neck function in cats (Vasavada et al. 1998), and neck and other musculoskeletal functions in humans (Keshner et al. 1997; Yamaguchi 2001).

Muscles of extant vertebrates must produce force to maintain posture, which diminishes the amount of force available to perform positive work. However, ligaments can contribute

substantially to maintaining posture against gravitational loads. Hengst (2004) noted that interspinous ligaments of many tetrapods support the tail, trunk, neck, and head against gravity, often with high safety factors. In these animals muscular effort is unnecessary for holding the head and neck in a neutral or ventroflexed posture. Muscles must, therefore, overcome the inertia of the head and neck when accelerating them, but need not overcome gravitational acceleration on these structures (Hengst 2004).

Large and rugose interspinous ligament scars in *Tyrannosaurus rex* (AMNH 5027) indicate that large and strong ligaments were present, but do not conclusively demonstrate that these ligaments eliminated the need for muscular effort to maintain neck posture. We therefore use data from ligament scars, ligament material properties, and inertial properties of the *T. rex* head and neck to assess whether its neck ligaments were able to support the feeding apparatus passively.

Institutional Abbreviations.—AMNH, American Museum of Natural History, New York; BM(NH), Natural History Museum, London; BHI, Black Hills Institute of Geological Research, Hill City, South Dakota; BMR, Burpee Museum of Natural History, Rockford, Illinois; CMN, Canadian Museum of Nature, Ottawa; FMNH, Field Museum of Natural History, Chicago; MOR, Museum of the Rockies, Bozeman, Montana; ROM, Royal Ontario Museum, Toronto.

Materials and Methods

Modeled Specimen

The specimen chosen for dynamic modeling was *Tyrannosaurus rex* AMNH 5027. The skull, anterior thoracic vertebrae, and cervical ribs were all modeled. Vertebrae C2–C10 and D1 were based entirely on this specimen. The non-intercentrum elements of C1 appear anteroposteriorly compressed compared with those of other tyrannosaurid atlas specimens, and these were partially reconstructed on the basis of *Tyrannosaurus rex* BM(NH) R7994, FMNH PR2081, MOR 555, and BMR 2002.4.1. AMNH 5027 was selected as the subject for modeling for five reasons: (1) The presacral axial skeleton of the specimen is complete. (2) Thanks to Carl Mehling and the AMNH, the mount was examined and photographed from a cherry picker, which permitted direct lateral and elevated views. (3) Casts of the mount are common, and repeated, close examination of the skull and individual vertebrae were possible at BMR, CMN, and ROM. (4) Accurate lateral and dorsal figures of the specimen by Paul (1988) require little modification for dynamic modeling. (5) Finally, the specimen was fully adult when it died, and muscle attachments are generally unambiguous.

Construction of Computational Models

Reconstruction of Osteological Morphology and Orientation of the Head-Neck System.—The specimen was represented in 3-D Cartesian coordinate space, with lateral and dorsal images of the skull and vertebrae C1–D1 overlain onto grids with units in centimeters. The point $[x, y, z] = [0, 0, 0]$ of the coordinate space was set to the posteroventral extremity of the first dorsal vertebra D1. The x-axis defined the anteroposterior dimensions of the restoration, the y-axis the dorsoventral dimensions, and z coordinates describe the mediolateral dimensions. The bones were traced in Adobe Illustrator®, from specimen photographs or drawings by Gregory Paul, on loan to D. M. Henderson. The drawings were scaled to measurements of the specimen, and modified to fit these measurements to correct for perspective and taphonomic distortion. The cranium of the specimen is taphonomically distorted, with the quadratojugal and squamosal disarticulated on the right side. The left side is comparatively uncrushed, however. Measurements incorporating osteological landmarks on the left side invariably confirmed the accuracy of Gregory Paul's drawings to within less than 3%.

Because individual bones were represented in lateral and dorsal views, their reconstructions could be manipulated via translation and rotation functions in Adobe Illustrator®. Each element, therefore, could move in three translational directions and around three axes of rotation, for a total of 66 degrees of freedom (C1–10 plus the skull about the atlanto-occipital joint). Each segment was treated as a rigid

body that geometrically defines its own reference frame (Yamaguchi 2001), which simplifies the assignment of rotational axes.

Dorsoventral centers of rotation were estimated after the results of Selbie et al. (1993), who determined through sophisticated mathematical methods the axes of dorsoventral intervertebral rotation in the cat. This axis was usually at a position approximately 60% of the centrum height of the anterior vertebra of each pair, and within the intervertebral disk between the vertebrae. This finding (Selbie et al. 1993) may be initially counterintuitive, and tyrannosaurids and cats are phylogenetically distant. However, other possible axes of rotation (such as at the zygapophyses, neural canal, within either centrum, or at the ventral base of either centrum) resulted in excessive disarticulation of centra and/or zygapophyses in the tyrannosaurid model.

Vertical axes for lateral rotation were assumed to be through the neural spine of the anterior vertebra of each pair. This almost invariably coincided with the midpoint between the prezygapophyses of the posterior vertebra. This axis of rotation would have allowed the maximum angular displacement possible by the 50% rule of zygapophyseal overlap (Stevens and Parrish 1999).

Movement of each element relative to adjoining structures was constrained through measurement and manipulation of casts of specimens (AMNH 5027, BHI 3033). Three assumptions guided estimates of maximal range of motion: (1) Overlap between adjoining articular surfaces (zygapophyes and the atlantooccipital articulation) was allowed to fall to 50% of the appropriate dimension of the smaller facet (Stevens and Parrish 1999). (2) Disarticulation of joint surfaces was not allowed to cause other structures of the bones (such as transverse processes and prezygapophyseal laminae) to come into contact. (3) Distances between muscle origins and insertions were not allowed to exceed 130% of the muscle/tendon length in the initial neutral posture. The last two assumptions sometimes placed tighter constraints on range of motion than the maximum extent possible through the 50% rule of zygapophysis disarticulation (Stevens and Parrish 1999).

The neck and skull of *Tyrannosaurus rex* (AMNH 5027) were represented in four different postures: a neutral to slightly elevated pose (Paul 1988), a highly dorsiflexed posture, maximum ventroflexion, and with the head turned laterally to an angle 60° from the midsagittal plane (but in a dorsoventrally neutral posture). In all of these postures, the ventral surfaces of C10 and D1 are parallel to the ground, which simplifies positioning the origin of the global coordinate system in dorsal and lateral views. This relationship would occur in life only when the preacetabular portion of the body was elevated by approximately 10°, because the back sloped downward when the body was passively cantilevered over the hips. In future studies a correction factor of −10°, or others for testing other postures, can be applied to calculated muscle lines of action.

Specification of Muscle Geometry.—Muscle origins and insertions were specified on the basis of tyrannosaurid muscle reconstructions (Table 1, Fig. 1A) (Snively 2006; Snively, Russell, and Powell unpublished). Smaller attachments were simplified as 4-cm-diameter dots at the approximate centroids of their anatomical position on the bones. The insertion of M. complexus and the dorsoventral extent of the M. longissimus capitis superficialis insertion are fairly large and were represented as thick lines that covered the areas of the insertions. These lines were approximated as four equally spaced points. The insertion of M. longissimus capitis superficialis is comparatively narrow, however, and was modeled as such in dorsal view.

In some cases muscles would not have had a direct line of pull from origin to insertion, and instead tendons ran over points in a pulley-like arrangement. This occurred with tendons of M. transversospinalis cervicis and M. transversospinalis capitis, because in most postures the neck is strongly curved in the midsagittal plane. As in birds, multiple tendons of M. transversospinalis cervicis (inserting onto the anterior epipophyses) ran between the epipophysis and neural arch of the vertebra just posterior to the insertion. Single, broad tendons of M. transversospinalis capitis ran over each side of the broad spine tables of

C2 and C3. Additionally, when the head and neck were lateroflexed, some muscles on the extended side (opposite the side of acute flexure) did not have an unobstructed line of pull from their origins to the head.

The solution to obstructed lines of pull is the adoption of points through which muscle force was channeled, called ''via points'' after Delp and Loan (1995). These are analogous to points on the wheels of a pulley, and, aside from negligible friction, the muscle's full tension is transmitted through the via points to the insertion. Kinematically they serve as effective positions of origin for the muscle force acting on the insertion. As with true muscle origins, via points were positioned in 3-D global coordinate space.

The average line of pull of a muscle, from insertions or via points, was estimated by simple vector addition. The point at the centroid of each muscle insertion or via point was considered the origin (0, 0, 0) of a set of position vectors, running from this point to the respective muscle origins at points (i_x, i_y, i_z). These vectors were summed, such that the angles of pull (α) relative to any of the universal coordinate axes can be calculated as in equation (3):

$$\alpha = \tan^{-1} \sum i / \sum (i_x, i_y, i_z) \qquad (3)$$

where i in the numerator is the sum of either x, y, or z dimensions. These angles, relative to any of the coordinate axes, were not necessary for calculating effective pull of each muscle, because each muscle insertion defines its own reference frame. The vector sum Σ (i_x, i_y, i_z) was taken as defining the overall direction of pull of the muscle relative to its local coordinate ''origin.''

This calculated line of pull is subject to a major simplifying assumption. For muscles with multiple origins, position vectors from the insertion to each origin represent equivalent contributions to the cross-sectional area of a given muscle, and hence equivalent contribution to the muscle's force. The position vectors are not force vectors themselves, but instead geometrically describe sets of fascicles that contribute equally to force. This assumption undoubtedly does not describe muscle architecture in *Tyrannosaurus rex* with complete accuracy, but is reasonable for three reasons. First, to assign different force contributions to fascicles arising from different origins would introduce additional assumptions in each case. Second, not enough is known or deducible about individual *T. rex* neck muscles to gauge the accuracy of the additional assumptions, and the high number of origins for many muscles would make sensitivity analyses unwieldy. Third, if a muscle's architecture is established as a Level I' inference in *T. rex* by extant phylogenetic bracketing (Witmer 1995), correction factors can be applied easily to (i_x, i_y, i_z) in equation 3.

Determination of Effective Muscle Pull.—The capacity of a muscle to generate torque will be proportional to the force it exerts in a direction orthogonal to its moment arm, from the joint's center of rotation to the muscle's insertion. The muscle's contribution to the system's torque will be the total force it generates multiplied by the cosine of the angle θ between two vectors: that of the muscle's line of pull (p), and a vector orthogonal to the moment arm (o). This cosine can be calculated by rearranging the expression for the dot product between the vectors:

$$\cos \theta = p \cdot o / \|p\| \|o\| \qquad (4)$$

in which $p = (x_p, y_p, z_p)$ and $o = (x_o, y_o, z_o)$, whose distances from their common origins (calculated and multiplied together in the denominator) are defined as $\sqrt{x^2 + y^2 + z^2}$.

Muscle Moments

Moment-generating capacities of muscles with systematically determinable cross-sectional areas and moment arms were estimated for *Tyrannosaurus rex*. These moments are not constant for a given muscle, but instead vary with posture as origins and insertions shift in distance and angular relationships relative to each other. Moment- or torque-generating capacities of the muscles (τ_m) were calculated as the cross product of muscle force F_m and moment arm R:

$$\tau_m = R \times F_m = RF_m \sin \phi. \qquad (5)$$

The angle ϕ is that between the vectors R and F_m, with their tails at the same point (Halliday et al. 1994). This angle is 90° and $\sin \phi = 1$ in all cases here, because the component of the mus-

cle's force F_m perpendicular to the moment arm was calculated using equation (4). As in equation (2), F_m is the product of its physiological cross-sectional area and specific tension (physiological force-generating capacity):

$$F_m = \text{PCSA} \times \text{ST}. \quad (6)$$

Concentric and isometric ST were assigned as 24 and 30 $\text{N} \cdot \text{cm}^{-2}$, respectively (Keshner et al. 1997; Johnston 1985). Eccentric ST was assigned at 40 and 48 $\text{N} \cdot \text{cm}^{-2}$ to cover variance in concentric force (Keshner et al. 1997; Bamman et al. 2000).

Physiological cross-sectional area varies with muscle mass, average fascicle length, pennation angle, and density (Richmond 1998). PCSA is close to the anatomical cross-sectional area (ACSA) in muscles with little pennation (Bamman et al. 2000). As a simplifying assumption we treat tyrannosaurid muscles as having had a parallel fiber architecture, and to calculate their force we used ACSA as a proxy for PCSA in equation (6). This yields the minimum force the muscles could produce, because highly pennate architecture would increase PCSA.

We used three methods to estimate muscle anatomical cross-sections and tensions: (1) extant tendon-muscle correlation, (2) tendon safety factor, and (3) dry neck slicing. Not all methods were applicable to all muscles, but they could be used in concert to constrain possible cross-sectional areas.

1. Extant tendon-muscle correlation (ETMC). If data were available from extant archosaurs relating a given muscle's cross-sectional dimensions to the linear dimensions of the attachment area, the same proportions were assumed for the muscle in *T. rex*. This was possible for only two muscles, M. transversospinalis capitis and M. longissimus capitis superficialis.

In dissected specimens of juvenile *Alligator mississippiensis* and adult *Caiman crocodylus*, M. transversospinalis capitis (M. trans. cap.) is about five times as deep and twice as wide as the tendon of insertion, and M. longissimus capitis superficialis (M. long. cap. sup.) is about 1.5 times as deep and four times as wide. These dimensions correspond to those implicated by Cong et al. (1998) for *Alligator sinensis*, but the width relative width of M. transversospinalis capitis in dissected alligatorids was greater than figured by Seidel (1978) and Frey (1988). For the *T. rex* specimen, origin sizes of M. long. cap. sup. and size and rugosity of M. trans. cap. insertions suggest that the muscles were relatively bigger than in crocodilians. In the absence of other information, muscles dimensions relative to tendons in dissected animals were assumed for the muscle cross-sections in *T. rex*.

Externally the dimensions of these muscles were unconstrained, but they were constrained by deeper muscles from bulging proximally toward the vertebral column. Each area was therefore first approximated as that of a flattened superellipse (Motani 2001), with an exponent k of 2.5 governing the form of its curvature (an unflattened ellipse has an exponent of 2). Using the derivation in Snively (2006) and Snively, Russell, and Powell (unpublished), we can calculate the superellipse areas can be calculated with the constant in equation (7):

$$A_{\text{SE}} = 0.830284077 \times 4^{1-1/k} ab\sqrt{\pi} \quad (7)$$

in which a and b are semi-major and semi-minor axes and $k = 2.5$.

Dimensions of M. trans. cap. and M. long. cap. sup. derived from crocodilians were also used in the dry neck slicing method. With ACSA calculated using these methods, forces at various specific tensions were estimated using equation (6).

2. Tendon safety factor (TSF) method. Biewener (by personal communication in Carpenter and Smith 2001) suggested that tendons can withstand a tension three times that of the maximum isometric tension generated by the attached muscle. This safety factor can be used to estimate the force of muscles with tendinous insertions (such as the human or tyrannosaurid M. biceps brachii [Carpenter and Smith 2001]).

Muscles with discrete tendinous insertions in *T. rex* include M. trans. cap., M. trans. cerv., M. long. cap. sup., M. long. cap. prof., and M. r. c. v. The method is not useful for muscles with fleshy or aponeurotic attachments, whose ACSA had to be estimated using method 3.

The isometric tension of tendinous muscles

(F_m) was estimated as one-third of the tendon's ultimate tensile breaking load, the product of its ultimate tensile strength $(\text{UTS})_t$ and the cross-sectional area of the insertion (a_t) (equation 8).

$$F_m = \text{UTS}_t \times a_t/3. \quad (8)$$

The tensile strength of tendon varies with strain rate (increasing under more rapid loadings [Ng et al. 2004]), and between different tendons. However, for large, healthy tendons, UTS_t has consistently been calculated as approximately 100 megapascals (MPa) (e.g., 85–108 MPa [Gordon 1978; Pearsall et al. 2003]; 99 ± 12.2 MPa [Schechtman and Bader 2002]). 100 MPa is therefore realistic for UTS_t of tendons in *T. rex*, and was applied to equation (8). Tendon insertion areas were determined by tracing them, from scanned or digital photographs, in Adobe Illustrator®, scaling them in ImageJ, and calculating the scaled areas with that program. The values were used for a_t of each muscle in equation (6).

3. Dry neck method. This method is less precise than the others but is necessary for estimating cross-sections and tensions of muscles without discrete tendinous attachments. It is similar to the dry skull method of Rayfield et al. (2001) and Wroe et al. (2005), in which available expansion areas of jaw muscles were used as proxies for ACSA.

For calculation of areas by the dry neck method, muscles were drawn surrounding anterior views of vertebrae or the occiput in Adobe Illustrator®. Their morphology was guided by bracketed muscle reconstructions, lines of action calculated herein, cross-sectional calculations for some muscles by method 1, and constraints of surrounding bones and muscles. Fortuitously, many muscles were constrained by the superficial muscles M. long. cap. sup. and M. trans. cap. For example, in crocodilians M. trans. cerv. does not encroach dorsally above the neural spine origins of M. trans. cap., and M. long. cap. prof. does not laterally displace the insertion tendon of M. long. cap. sup. The same constraints were assumed for *T. rex*. The cross-sectional areas of muscles were estimated by the same procedure as used for tendon areas in the TSF method, and these figures for ASCA were used for force calculations in equation (6).

In *T. rex* AMNH 5027 the insertion of M. spl. cap. is round in cross-section. It was assumed that the muscle's diameter did not exceed that of this insertion, and that its cross-sectional area (πr^2) was no greater than that of its inferred circular insertion.

Interspinous Ligament Moments and Rotational Inertias of the Feeding Apparatus

Ligament ultimate and resisted gravitational moments were calculated for ligaments between C9 and C10, C5 and C6, and the axis and skull, with methods detailed by Snively (2006) and Snively, Russell, and Powell (unpublished). The greatest moment that an interspinous ligament can withstand before failure, as it resists a force anterior to it, is calculated using equation (9).

$$F_L \times r_L = F_g \times r_g. \quad (9)$$

F_L is the ligament's ultimate stress (58 MPa [Provenzano et al. 2002]) times its cross-sectional area, and r_L is the distance from the center of the ligament to a point just above the neural canal. Cross-sectional areas were taken to be the average of ligament scar areas in the specimen (treated as ellipses, with major and minor radii measured with calipers), multiplied by the amount the areas would diminish to (0.895) under ligament's failure strain of 12.5% and Poisson's ratio of 0.45 (Provenzano et al. 2002). To avoid permanent deformation, $F_L \times r_L$ must equal or exceed the force the ligament cantilevers (F_g) multiplied by the distance r_g from that force to the ligament. Gravitational moment arms (r_g), from each interspinous ligament to the center of mass of structures anterior to it, were calculated along with rotational inertias of the feeding apparatus, using 3-D computer models of the head and neck (Fig. 1B–D).

These computer models were constructed by mathematically combining outlines of dorsal and lateral flesh reconstructions (Henderson 1999; Henderson and Snively 2003). Dorsal and lateral outlines were subdivided into an equal number of segments (''slices''), with lines drawn through the outlines at equivalent positions along the body in each view. Vol-

umes of segments were calculated by integration, and their masses calculated by multiplying the volumes by assigned densities of each slice. Most segments of the head and neck were assigned the density of water, with a volume anterior to the braincase (pneumatized and not filled with bone or muscle) modeled with three possible densities, 1, 0.5, and 0.00129 times that of water. The last density is that of air at standard pressure and temperature. Because the prethoracic vertebrae of *Tyrannosaurus rex* were highly pneumatized (Brochu 2003; Wedel 2004), a density coefficient of 1 for the neck is a conservative overestimate.

Muscular Accelerations of the Feeding Apparatus

The capacity of each muscle to accelerate the feeding apparatus was assessed, in the neutral posture and at each extreme position of the head and neck (maximum dorsiflexion, ventroflexion, left and right lateroflexion). The angular acceleration (α_m) a muscle would produce can be calculated using equation (10):

$$\alpha_m = \tau_m / I. \tag{10}$$

Here τ_m is the torque the muscle produces, as calculated in equation (5), and I is the rotational inertia of the system. Rotational inertia was calculated using 3-D models (Fig. 1) with equation (11),

$$I = \sum_i m_i r_i^2 \tag{11}$$

in which m_i is the mass of a given segment i, and r_i^2 is the square of its distance from the axis of rotation of the system. The sum of $m_i r_i^2$ for all segments gives the rotational inertia.

When multiple muscles apply torques to accelerate a structure, angular accelerations are additive, so that the total acceleration α_t is calculated by equation (12),

$$\alpha_t = \sum_1^i \alpha_m \tag{12}$$

in which the number of muscles ranges from 1 to i.

Equation (10) gives α_m in radians/s^2. These units are useful for comparing abilities of muscles to accelerate segments of the body, but are not necessarily intuitive for judging how rapidly *T. rex* could move its head and neck. Using equation (13), α_m is easily convertible into tangential acceleration (a_m), at any point at any distance (r) from the center of rotation:

$$a_m = \alpha_m \times r. \tag{13}$$

Other angular and tangential quantities are easily calculated if α_t and the angular excursion θ are known. For example, the time over which the acceleration occurred and the angular velocity (ω) can be calculated by rearrangement and substitution in the following equations, assuming initial displacement and velocity are 0:

$$\theta = \alpha_t t^2 \tag{14}$$

$$\omega = \alpha_t t. \tag{15}$$

Tangential velocity (v_r) at distance r from the center of rotation is related by equation (16):

$$v_r = \omega r. \tag{16}$$

Results

Osteological Orientation and Muscle Lines of Action

Figures 2–6 depict muscle lines of action with the head and neck held in neutral, ventroflexed, dorsiflexed, and lateroflexed postures. Online supplementary tables (http://dx.doi.org.10.1666/06059.s1) list quantities for determination of muscle pull direction. These include position vectors for muscles in their local reference frames, vectors orthogonal to muscle moment arms, and cosines between these vectors (calculated with equation 4). Cosines are high overall for all postures, except for posteriorly originating muscles in the lateroflexed posture. M. longissimus capitis superficialis and M. iliocostalis capitis diminish most in effectiveness in this posture. Cosines for dorsi- and lateroflexive muscles are notably high with the neck and head dorsiflexed, indicating high muscle effectiveness when the head and neck were positioned high or extended anteriorly after dorsiflexion.

Muscle Moments

The above-mentioned torques incorporate cosines for effective muscle pull, estimated

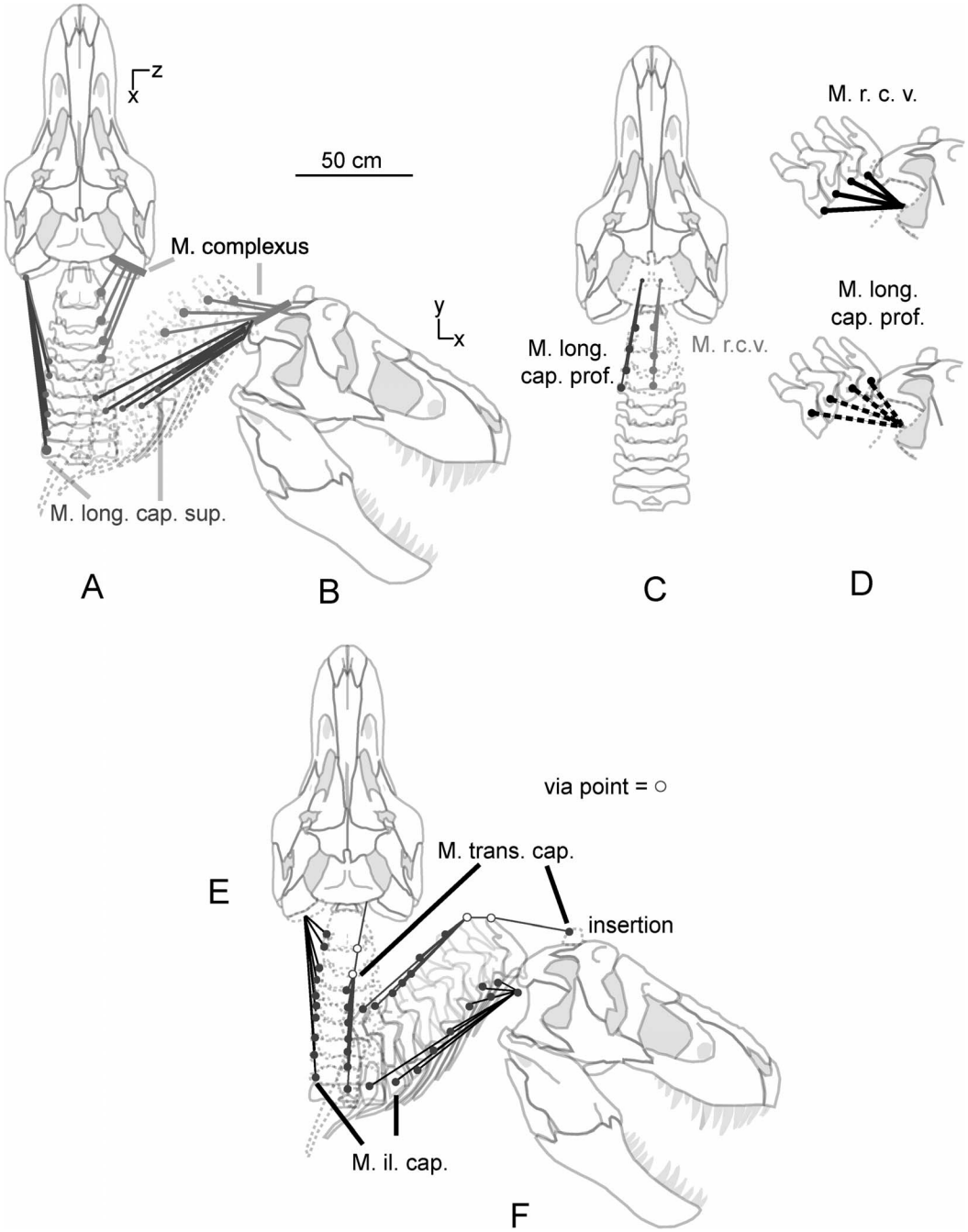

FIGURE 2. Position vectors of major neck muscles in *Tyrannosaurus rex* (AMNH 5027; skeletal drawings modified from Paul 1988), with the neck in a neutral to slightly elevated posture. Note that 3-D summation of these vectors yields direction for lines of muscle pull. Muscle abbreviations, origins, and insertions are as listed in Table 1; dots indicate attachment sites and via points. The top figure shows the scale, and vector axes in the frontal and sagittal planes. A, C, and E depict the skeleton and lines of action in dorsal view, and B, D, and F show these in lateral view. In B and E, bones of the neck are shown as dashed lines so that muscle lines of action are not obscured. In C and D, bones are shown as dashed lines to indicate that M. r. c. v. passes ventral or medial to them. A, B, M. longissimus capitis superficialis (M. long. cap. sup.: dark lines) and M. complexus (lighter-shaded lines). C, D, M. longissimus capitis profundus (M. long. cap. prof.; dashed black lines in D) and M. rectus capitis ventralis (M. r. c. v.). E, F, M. transversospinalis capitis (M. trans. cap.: dark gray lines) and M. iliocostalis capitis (M. il. cap.: black lines).

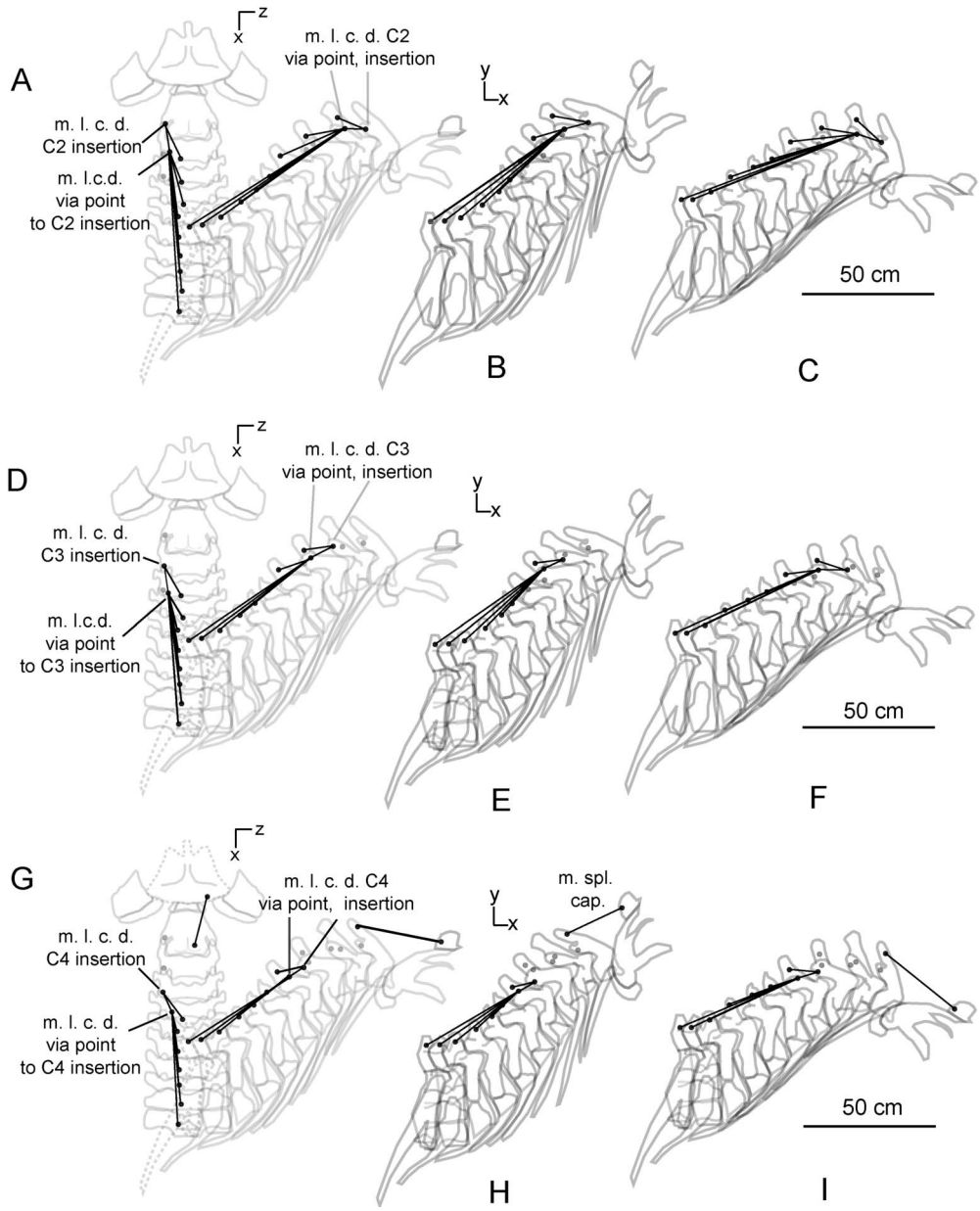

FIGURE 3. Position vectors for M. transversospinalis cervicis (M. trans. cerv.), inserting on the epipophyses of C2 (A, B, C), C3 (D, E, F), and C4 (G, H, I) of *Tyrannosaurus rex* (AMNH 5027; skeletal drawings modified from Paul 1988), and of M. splenius capitis from the axis to the parietals (G, H, I). Note that via points proximal to insertions act as geometric ''origins'' of pull. Insertions and via points through which tendons ran are labeled in A, D, and G. Neutral/slightly elevated, dorsiflexed, and ventroflexed postures are shown from left to right in each sequence. The lateral z components (A, D, and G: dorsal views) were constant for calculating lateral flexion resultants in all postures, whereas x (anteroposterior) and y (dorsoventral) components varied with posture.

muscle forces, and moment arms. Table 2 lists forces calculated by the EMTC and DNM methods, and Tables 3 and 4 list inertias and gravitational moments that muscle moments had to overcome. Tables 5–9 list muscle moments calculated using equation (5). (Tables in the online supplementary information list all quantities necessary for calculating the moments, for all five tested postures.) Dorsiflexion and ventroflexion moments are listed with

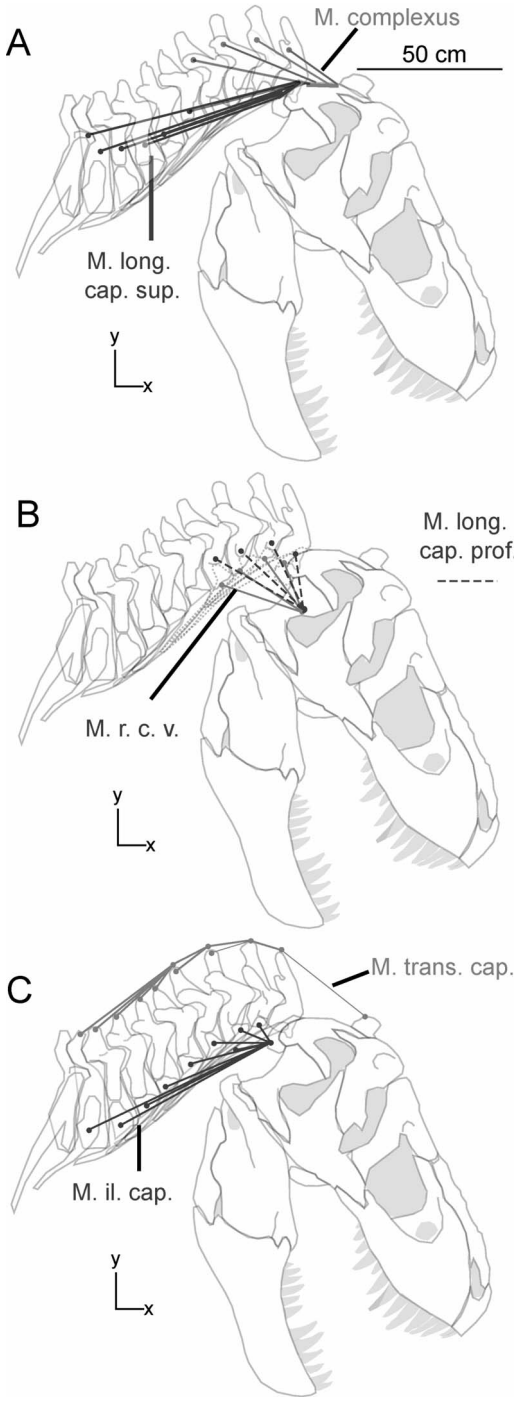

FIGURE 4. Position vectors for craniocervical muscles of *Tyrannosaurus rex* (AMNH 5027; skeletal drawings modified from Paul 1988) with the head and neck held in a ventroflexed posture. Note that the cranial ventroflexors (B) have their highest capacities for ventroflexive accelerations in this posture (Tables 8, 9). These lateral ordinations enable decomposition of *x* and *y* components; lateral (*z*) components are the same as in a neutral posture (Fig. 2). A, M. longissimus capitis superficialis (M. long. cap. sup.) and M. complexus. B, M. longissimus capitis profundus (M. long. cap. prof.) and M. rectus capitis ventralis (M. r. c. v.). C, M. transversospinalis capitis (M. trans. cap.) and M. iliocostalis capitis (M. il. cap.). Muscle vectors and bone outlines follow the shading and dash conventions of Figure 2.

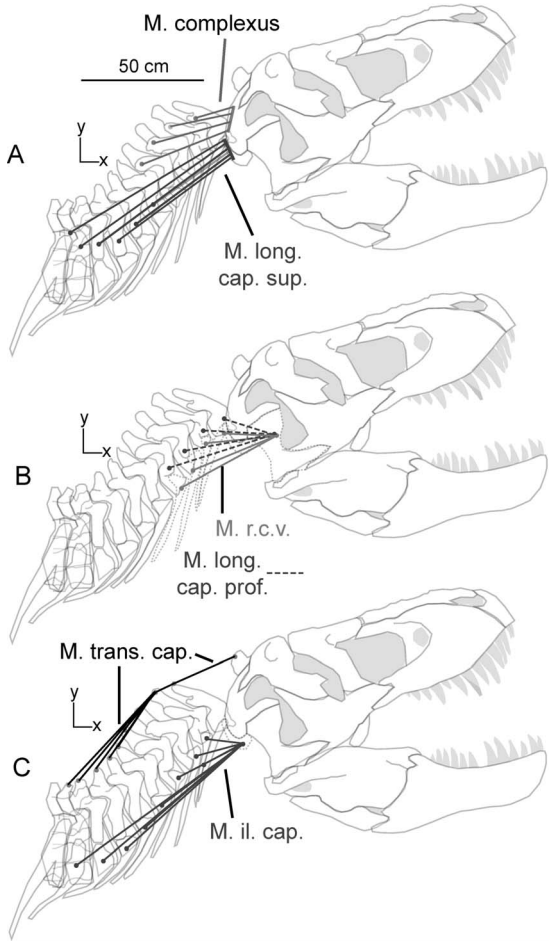

FIGURE 5. Position vectors for craniocervical muscles of *Tyrannosaurus rex* (AMNH 5027; skeletal drawings modified from Paul 1988) with the head and neck held in a dorsiflexed posture. Note that the parallel lines of pull for M. longissimus capitis superficialis would have enabled particularly forceful lateroflexion in this posture. These lateral ordinations enable decomposition of *x* and *y* components; lateral (*z*) components are the same as in a neutral posture (Fig. 2). A, M. longissimus capitis superficialis (M. long. cap. sup.) and M. complexus. B, M. longissimus capitis profundus (M. long. cap. prof.) and M. rectus capitis ventralis (M. r. c. v.). C, M. transversospinalis capitis (M. trans. cap.) and M. iliocostalis capitis (M. il. cap.). Muscle vectors and bone outlines follow the shading and dash conventions of Figure 2.

bilateral contraction of each muscle, and would be half the reported value with unilateral contraction.

The highest moments occurred for large muscles, with large moment arms and favorable lines of pull, especially for dorsiflexion by M. transversospinalis capitis and M. complexus, and lateroflexion by M. longissimus capitis superficialis when the head and neck were in a dorsiflexed posture. Moments scale linearly with specific tension and are greatest for eccentric contraction. The values for concentric moments are gauges of absolute and relative ability to accelerate the head, whereas eccentric values are indices (not necessarily absolute values) of ''braking torque'' that the muscles could apply to decelerate the feeding apparatus or tear flesh under high loadings.

Forces and moments calculated by the tendon safety factor (TSF) method were three to four times higher than those calculated using other means. For example, concentric force for M. transversospinalis capitis by this method is estimated at 45,000 N. Because these forces were so much greater than estimated from muscle cross-sectional reconstructions, the latter were taken to be reasonably conservative and were used for estimates of WGC and acceleration.

Muscle Work-Generating Capacity and Radial Accelerations of the Feeding Apparatus

Tables 3 and 4 detail rotational inertias along the neck and head of *Tyrannosaurus rex*, used for calculating radial accelerations by neck muscles. These rotational inertias of the entire feeding apparatus are for the neutral posture only. The head always had the listed rotational inertia for dorsiflexion, ventroflexion, and lateroflexion. However, angular deflections of the intercervical joints, and of the head on the neck, affected the rotational inertia of the entire feeding apparatus. Ventroflexion of the neck would lengthen the head plus neck and increase *I*, whereas latero- and dorsiflexion would decrease *I* below the values reported here.

Angular accelerations produced by all neck muscles for all tested postures are detailed in Tables 5–9; acceleration values indicate comparative work-generating capacities (WGC) of muscles under varying contractile conditions. Concentric values give reasonable accelerations of the head and neck when loaded only by their own rotational inertias. As for eccentric moment-generating capacity, eccentric ''accelerations'' are not realistic quantities, but are rather indices of WGC when the muscles are under a load that exceeds their concentric capabilities. WGC is linearly proportional to muscle specific tension. Accelerations of the head alone by concentric contractions are realistic in all postures. However, mass was brought closer to the base of the neck in other postures, diminishing rotational inertias (Carrier et al. 2001) and increasing the accelerative capacity of muscles that moved the neck plus head.

All radial accelerations are inversely proportional to rotational inertia, and linearly proportional to force and moment arm. Variation in cosines of muscle pull has a substantial effect on some accelerations. For example, favorably high cosines when the feeding apparatus is dorsiflexed leads to high dorsiflexive acceleration by M. transversospinalis capitis and high laterally flexive acceleration by M. longissimus capitis superficialis. Conversely, acceleration by M. longissimus capitis superficialis is weak in laterally flexed postures, when the neck is neutrally curved in the sagittal plane, but the head and neck are laterally flexed in the frontal plane. Unlike M. longissimus capitis superficialis, M. complexus retains high cosines for lateroflexion of the head in lateroflexed postures.

Interspinous Ligament Moments

Table 4 lists bending moments from C10 anteriorly up to C2, imposed by the mass anterior to each point, and the moment arm from each vertebra to the center of mass (c.m.) of the head plus neck anterior to it. Depending on the assigned antorbital density, ligament ultimate moments exceed gravitational moments by 14.1–15.2 for C9–C10, and 6.6–8.3 for C5–C6, and 4.8–5.5 for the putative C2-cranial ligament. Assuming that other neck ligaments of *Tyrannosaurus rex* had comparably high safety factors, interspinous ligaments obviated the need for muscular effort for maintaining head and neck posture.

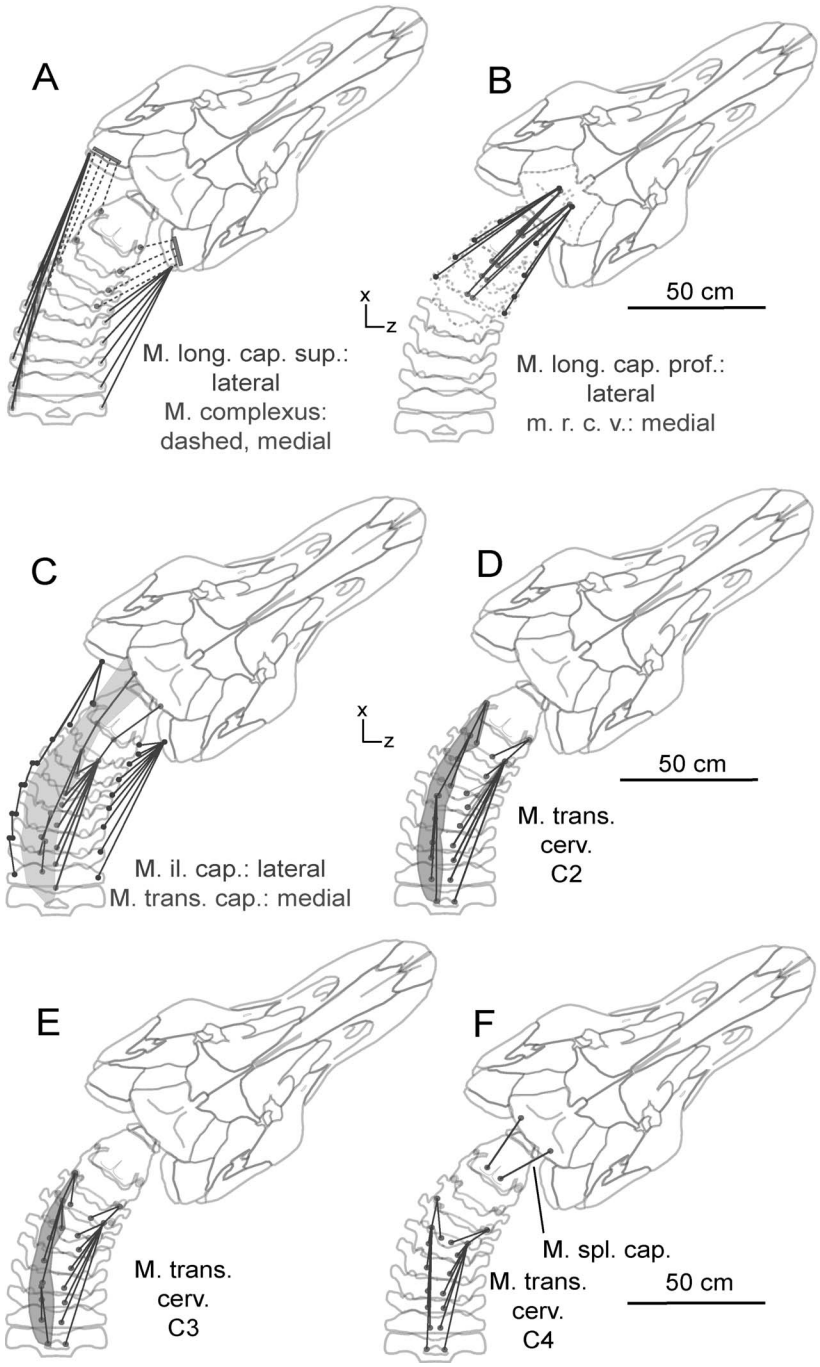

FIGURE 6. Position vectors for craniocervical muscles of *Tyrannosaurus rex* (AMNH 5027; skeletal drawings modified from Paul 1988) with the head and neck held in a lateroflexed posture in the frontal plane, with the same dorsoventral orientation as in a neutral posture. Note that M. complexus increases in lateroflexive capability in this posture compared with that of M. long. cap. sup. These dorsal ordinations enable decomposition of *x* and *z* components; vertical (*y*) components are the same as in the neutral posture (Fig. 2). Muscle vectors and bone outlines follow the shading and dash conventions of Figure 2. A, M. longissimus capitis superficialis (M. long. cap. sup.) and M. complexus. B, M. longissimus capitis profundus (M. long. cap. prof.) and M. rectus capitis ventralis (M. r. c. v.). C, M. transversospinalis capitis (M. trans. cap.) and M. iliocostalis capitis (M. il. cap.). For M. trans. cap., lines of tension on the left, extended side from fascicles posterior to C8 are considered as transmitted through via points within the muscle (represented as a transparent overlay). On both sides, the insertion tendon of M. trans. cap.

TABLE 2. Estimated cross-sectional dimensions and forces of neck muscles of *Tyrannosaurus rex* (AMNH 5027). Dimensions estimated by extant muscle-tendon size correlation (EMTC) for M. transversospinalis capitis and M. longissimus capitis superficialis, and by the dry neck slicing method (DNM) for other muscles. Areas calculated as superelipses. Concentric specific tension is 24 N/cm², isometric ST is 30 N/cm², and low and high eccentric ST are 40 N/cm² and 48 N/cm², respectively.

	M. trans. cap.	M. complexus	M. spl. cap.	M.trans. cerv.	M. long. cap. sup.	M. long. cap. prof.	M. il. cap.	M. r. c. v.
Muscle semi-major axis (cm)	12.5	10.36	5	6	11.5	10.021	6.85	11.07
Muscle semi-minor axis (cm)	7.5	7.4	5	4	7	2.97	6.249	3.39
Cross-sectional area (cm)	316.96	259.20	78.54	81.14	266.25	100.64	144.72	126.73
F: concentric (N)	7607.04	6220.72	1884.96	1947.42	6390	2415.40	3473.36	3041.61
F: isometric (N)	9508.8	7775.89	2356.2	2434.28	7987.50	3019.25	4341.70	3802.01
F: eccentric low (N)	12,678.4	10,367.86	3141.6	3245.70	10,650	4025.67	5788.94	5069.34
F: eccentric high (N)	15,214.08	12,441.43	3669.92	3894.84	12,780	4830.80	6946.73	6083.21

Results for Quantities and Hypotheses Related to Feeding Functions in *Tyrannosaurus rex*

Because these quantities are estimations for an extinct animal, they are rounded here to one decimal place, or to the nearest whole number for larger values. Tables listing the quantities give results to three decimal places.

Magnitude 1: Maximum Vertical Acceleration as the Head Passed through a Neutral Position.—This maximum angular acceleration in the sagittal plane is the sum of accelerations produced by the major head dorsiflexors, as formalized in equation (12). If ligamentous support was present, with summed muscle moment-generating capacity of 7164 Nm, the total angular acceleration α_t of the head was 147.4 rad/s². This translates into a tangential acceleration at the head's center of mass, c.m. (0.437 m anterior to the occipital condyle: Table 3) of 64.4 m/s², or 6.6 *g*. Because the eyes were only 0.27 m from the occipital condyle; the gaze would have shifted at a maximum tangential acceleration of 4.1 *g* as the head was dorsiflexed through the neutral posture.

These magnitudes do not diminish greatly if muscular effort must be assumed for maintaining head posture. The muscles would have to counteract a gravitational moment of 1152 Nm, reducing their concentric moment-generating capacity to 6012 Nm. In this case total angular acceleration (α_t) would have been 125 rad/s², for tangential accelerations at the head's c.m. and eyes of 5.5 *g* and 3.6 *g*, respectively.

Magnitude 2: Maximum Vertical Load.—The maximum load the neck dorsiflexors could have sustained under isometric contraction was 8956 Nm, and the maximum eccentric loads were 11,942 Nm and 14,330 Nm, depending on estimated eccentric force. At the position of the largest maxillary teeth (0.9 m from the occipital condyle), these moments would have enabled the *T. rex* to statically hold 1014 kg and set down maximum masses of 1353 and 1623 kg, respectively.

Magnitude 3: Maximum Lateral Acceleration.—The maximum lateral acceleration (α_t) of this *T. rex*'s head through its neutral position was the sum of acceleration of lateral flexors estimated by equation (12). If only major lateroflexors are considered (M. long. cap. sup., M. complexus, M. il. cap.), lateral acceleration was 70.3 rad/s², or 30.7 m/s² (3.1 *g*) and 19 m/s² (1.9 *g*) at the heads's c.m. and at the eyes, respectively. These values increase when lat-

←

passed through via points over the neural spines of C3 and C2. D, M. transversospinalis cervicis (M. trans. cerv.) inserting on C2. On the left (extended) side, tension from posterior fascicles is modeled as passing through intramuscular via points. The muscle is shown as a transparent overlay. E, M. trans. cerv. inserting on C3, with similar intramuscular via points and the muscle shown as a transparent overlay. F, M. trans. cerv. inserting on C4, and M. spl. cap.

TABLE 3. Quantities for calculating rotational inertias (I, right column) of the feeding apparatus of *Tyrannosaurus rex* (AMNH 5027). Masses and moment arms to centers of mass are given for regions anterior to vertebrae 1–9, with three estimated densities of the antorbital region from the braincase to the premaxillae. Note that rotational inertias of the head (anterior to vertebra 1) vary substantially depending on the assigned antorbital density.

Anterior to vert. no.	Moment arm (m)	Mass (kg)	I (kg·m²)
Antorbital density: 1000 kg/m³			
1	0.44	306.12	58.47
2	0.49	343.68	82.09
3	0.52	368.77	100.52
4	0.55	394.64	121.38
5	0.59	421.60	144.72
6	0.62	451.45	173.23
7	0.66	485.25	209.76
8	0.70	523.41	255.49
9	0.74	574.26	313.84
Antorbital density: 500 kg/m³			
1	0.43	295.01	53.49
2	0.48	332.57	75.67
3	0.51	357.66	93.06
4	0.54	383.53	112.80
5	0.57	410.49	134.97
6	0.61	440.34	162.12
7	0.64	474.13	197.02
8	0.69	512.29	240.84
9	0.73	563.15	296.91
Antorbital density: 0 kg/m³			
1	0.41	283.89	48.59
2	0.46	321.46	69.34
3	0.50	346.54	85.70
4	0.53	372.41	104.34
5	0.56	399.37	125.35
6	0.59	429.22	151.16
7	0.63	463.02	184.44
8	0.67	501.18	226.37
9	0.71	552.03	280.19

eral flexion by other muscles is added (to 92.7 rad/s²).

Magnitude 4: Maximum Lateral Load.—The maximum lateral moments that the lateral flexors could have withstood would be 4629 Nm under isometric contraction, and 5692 and 6831 Nm under estimated eccentric forces, when the head was held neutrally.

Hypothesis 1: Moment-generating capacity of head dorsiflexors increased as the head was dorsiflexed.—This hypothesis is falsified for the dorsiflexors M. trans. cap., M. complexus, and M. spl. cap. acting in concert. Total moment-generating capacity of dorsiflexors rises from 6912 Nm in the ventroflexed to 7165 Nm in the neutral posture, but then diminishes to 6265 Nm in the dorsiflexed posture.

TABLE 4. Gravitational moments on centers of mass anterior to vertebrae in *Tyrannosaurus rex* (AMNH 5027). Note that these moments had to be resisted by ligaments connecting each vertebral pair.

	Antorbital density (kg/m³)		
Ligament	1000	500	0
C1–ckull	−1312.41	−1232.31	−1152.21
C2–C3	−1647.77	−1556.19	−1464.62
C3–C4	−1888.78	−1789.68	−1690.59
C4–C5	−2147.03	−2040.42	−1933.8
C5–C6	−2423.18	−2309.04	−2194.9
C6–C7	−2743.39	−2621.1	−2498.81
C7–C8	−3129.73	−2998.27	−2866.81
C8–C9	−3587.38	−3445.83	−3304.28
C9–C10	−4164.64	−4011.38	−3858.12

Hypothesis 2: Moment-generating capacity of head lateroflexors increased from the point of maximum left lateral flexion to the neutral posture, and decreased as the head continued to be swept to the right.—Moment-generating capacities of lateroflexors display the same pattern as the dorsiflexors as the head was swept through the neutral posture. Total torques exerted by lateroflexors increase from 3245 Nm in the right-flexed posture to 3415 Nm in the neutral posture, and then diminish markedly to 2813 Nm in the left-extended posture.

Hypothesis 3: Craniocervical muscles of T. rex could impart sufficient acceleration to the head, neck, and a 50-kg bolus of food to conduct inertial feeding.—This hypothesis is testable using equations (11–16). With the center of mass of a bolus of food positioned between the large anterior maxillary teeth, 0.9 m from the occipital condyle, rotational inertia of the head plus food was 89 kg m². By concentric contraction of all dorsiflexors, the head plus food would be accelerating at 77.6 rad/s² in the ventroflexed posture, 80.4 rad/s² in the neutral posture, and 79 rad/s² in the dorsiflexed posture. Assuming an average acceleration of 79 rad/s², average tangential acceleration would be 7.2 *g*, with a total angular displacement of $\pi/4$ (0.7854) radians. It would take the head 0.1419 seconds to traverse this short angular distance at this average acceleration, leading to a terminal angular velocity of 11.1 rad/s. At 0.9 m from the center of rotation at the occipital condyle, the food would be traveling at a tangential velocity of 10 m/s, more than sufficient for toss-and-catch inertial feeding with

TABLE 5. Concentric accelerations and work-generating capacity (isometric and eccentric ''accelerations'') of the feeding apparatus of *Tyrannosaurus rex* (AMNH 5027), imparted by M. transversospinalis capitis (right columns). For neck dorsiflexion, the center of rotation (c.r.) is estimated to have been between vertebrae C7 and C6. Except for neck dorsiflexion, rotational inertia is 48.59 kg·m^2. Note that as reconstructed and when acting in dorsiflexion, M. transversospinalis capitis had the highest moment- and work-generating capacity of any *T. rex* neck muscle.

	M. transversospinalis capitis: accelerations			
	Moments: N·m		Accelerations: rad/s^2	
	L-flex.	D-flex. (bilat.)	L-flex.	D-flex. (bilat.)
Neutral pose				
Concentric	572.86	4612.6	11.789	94.923
Isometric	716.07	5765.8	14.736	118.65
Eccentric low	954.76	7687.7	19.648	158.21
Eccentric high	1145.7	9225.2	23.578	189.85
Dorsiflexed				
Concentric	578.24	4656	11.9	95.816
Isometric	722.81	5820	14.875	119.77
Eccentric low	963.74	7760	19.833	159.69
Eccentric high	1156.5	9312	23.8	191.63
Ventroflexed				
Concentric	557.33	4487.6	11.469	92.351
Isometric	696.67	5609.5	14.337	115.44
Eccentric low	928.89	7479.4	19.116	153.92
Eccentric high	1114.7	8975.2	22.939	184.7
Flexed right side				
Concentric	408.73	3291.1	8.4113	67.727
Isometric	510.91	4113.8	10.514	84.659
Eccentric low	681.22	5485.1	14.019	112.88
Eccentric high	817.46	6582.2	16.823	135.45
Extended left side				
Concentric	448.27	3609.4	9.225	74.279
Isometric	560.34	4511.8	11.531	92.849
Eccentric low	747.11	6015.7	15.375	123.8
Eccentric high	896.54	7218.9	18.45	148.56
Neck dorsiflexion (c.r. between C7 and C6; I =1 84.4 kg·m^2)				
Concentric		4107.8		22.271
Isometric		5069		27.483
Eccentric low		6758.7		36.644
Eccentric high		8110.4		43.972

a 50-kg bolus of food. With a flip of the head alone at maximum force of the dorsiflexors, at this tangential velocity the food would travel 5 m into the air.

Accelerations of the entire feeding apparatus by neck and head dorsiflexors were slower, but could have achieved substantial tangential velocities of the food. Rotational inertias of the feeding apparatus plus food overcome by M. trans. cerv., with the food at varying radii anterior to centers of intervertebral rotation, were 142 kg m^2 (anterior to C2), 172 kg m^2 (C3), and 199 kg m^2 (C4). Dividing muscle moments by these rotational inertias using equation (11), and adding the resulting accelerations, gives an acceleration of the head, neck, and food anterior to C3 of 8.1 rad/s^2. When the head was already dorsiflexed, M. trans. cap. and M. l. c. s. could have acted to dorsiflex the entire feeding apparatus. Rotational inertia of the head plus neck anterior to the C7–C6 point of rotation by M. trans. cap. was 184 kg m^2, and that of 50 kg of food 1.28 m anterior to this point was 82 kg m^2, for a total I of 266 kg m^2. With a moment of 4108 Nm exerted by the muscle on the feeding apparatus anterior to the center of rotation, equation (11) yields an angular acceleration of 15.42 rad/s^2. Total angular acceleration α_t by these muscles on the head was 23.6 rad/s^2, imparting a tan-

TABLE 6. Concentric accelerations and work-generating capacity (isometric and eccentric ''accelerations'') of the feeding apparatus of *Tyrannosaurus rex* (AMNH 5027), imparted by M. complexus and M. splenius capitis. Rotational inertias are 48.59 kg·m². Note that M. complexus had high potential accelerations for lateroflexion on the flexed (''right'') side, with the head in a lateroflexed posture.

	M. complexus				M. splenius capitis			
	Moments: N·m		Accelerations: rad/s²		Moments: N·m		Accelerations: rad/s²	
	L-flex.	D-flex. (bilat.)	L-flex.	D-flex. (bilat.)	L-flex.	D-flex. (bilat.)	L-flex.	D-flex. (bilat.)
Neutral pose								
Concentric	1458.9	1750.7	30.0	36.0	92.9	801.6	1.9	16.5
Isometric	1823.6	2188.4	37.5	45.0	116.1	1002.0	2.4	20.6
Eccentric low	2431.5	2917.8	50.0	60.0	154.9	1336.0	3.2	27.5
Eccentric high	2917.8	3501.4	60.0	72.1	180.9	1560.7	3.7	32.1
Dorsiflexed								
Concentric	1340.6	1608.7	27.6	33.1	89.4	771.2	1.8	15.9
Isometric	1675.7	2010.8	34.5	41.4	111.7	964.1	2.3	19.8
Eccentric low	2234.3	2681.1	46.0	55.2	149.0	1285.4	3.1	26.5
Eccentric high	2681.1	3217.4	55.2	66.2	174.1	1501.6	3.6	30.9
Ventroflexed								
Concentric	1352.1	1622.5	27.8	33.4	92.9	801.9	1.9	16.5
Isometric	1690.1	2028.1	34.8	41.7	116.2	1002.3	2.4	20.6
Eccentric low	2253.5	2704.1	46.4	55.6	154.9	1336.4	3.2	27.5
Eccentric high	2704.1	3245.0	55.6	66.8	181.0	1561.2	3.7	32.1
Flexed right side								
Concentric	1539.0	1846.8	31.7	38.0	83.3	718.4	1.7	14.8
Isometric	1923.8	2308.5	39.6	47.5	104.1	898.0	2.1	18.5
Eccentric low	2565.0	3078.0	52.8	63.3	138.8	1197.4	2.9	24.6
Eccentric high	3078.0	3693.6	63.3	76.0	162.1	1398.7	3.3	28.8
Extended left side								
Concentric	1273.2	1527.9	26.2	31.4	84.3	727.0	1.7	15.0
Isometric	1591.5	1909.8	32.8	39.3	105.3	908.8	2.2	18.7
Eccentric low	2122.0	2546.4	43.7	52.4	140.5	1211.7	2.9	24.9
Eccentric high	2546.4	3055.7	52.4	62.9	164.1	1415.5	3.4	29.1

gential acceleration to the food of 30.2 m/s² when the head was fully dorsiflexed. Inertial feeding was, therefore, possible by neck dorsiflexion alone, as well as by head dorsiflexors.

Discussion

Benefits of the Present Method for Estimating Musculoskeletal Dynamics

The algorithm used here for reconstructing *T. rex* neck dynamics has several practical and mathematical advantages. First, hypotheses are based on behavior of extant analogues with homologous muscles and musculoskeletal posture. Second, the method relies on physical measurements of specimens, uses accurately scaled dorsal and lateral diagrams to obtain 3-D vectors, and builds on muscle reconstructions that are as detailed and rigorous as possible. Third, the vector mathematics simplifies several calculations. For example, use of the dot product to determine cosines between vectors in 3-D yields muscle tension orthogonal to moment arms. This immediately gives relevant muscle tension without having to specify the angle between the muscle resultant and the vector orthogonal to the lever arm. It also simplifies calculation of moments by equation (5) because the angle between the relevant tension and the moment arm itself is 90°, with $\sin \phi = 1$. Fourth, specifying each muscle insertion as the origin of its own reference frame allows intuitive calculations of muscle effects at each joint (Yamaguchi 2001). The method is at a mathematical disadvantage to the partial velocity method, because it does not yield generalized equations of motion (Yamaguchi 2001).

TABLE 7. Concentric accelerations and work generating capacity (isometric and eccentric ''accelerations'') of the feeding apparatus of *Tyrannosaurus rex* (AMNH 5027), imparted by M. transversospinalis cervicis (two right columns). Rotational inertias vary, because centers of rotation are just posterior to the vertebrae of insertion. Note that radial accelerations for bilateral dorsiflexion (right column) were low, but substantial tangential accelerations were possible at the rostrum because radii of rotation were large.

	Moments: N·m		Accelerations: rad/s²	
	L-flex.	D-flex. (bilat.)	L-flex.	D-flex. (bilat.)
M. transversospinalis cervicis C2 insertion				
			I = 85.7 kg·m²	
Concentric	175.34	382.55	2.0459	4.4638
Isometric	219.17	478.19	2.5574	5.5798
Eccentric low	292.23	637.59	3.4099	7.4397
Eccentric high	350.67	765.1	4.0918	8.9277
M. transversospinalis cervicis C3 insertion				
			I = 104.34 kg·m²	
Concentric	175.34	450.61	1.4395	4.3186
Isometric	219.17	563.27	1.7994	5.3982
Eccentric low	292.23	751.02	2.3992	7.1976
Eccentric high	350.67	901.23	2.8791	8.6372
M. transversospinalis cervicis C4 insertion				
			I = 125.35 kg·m²	
Concentric	163.16	554.13	1.3017	4.4208
Isometric	203.95	692.66	1.6271	5.526
Eccentric low	271.93	923.55	2.1695	7.368
Eccentric high	326.32	1108.3	2.6033	8.8416

General Limitations of the Method and Potential Sources of Inaccuracy

Several assumptions necessary for this method will lead to varying degrees of error during calculation of musculoskeletal dynamics. As long as skeletal measurements, photographs, and accurate skeletal drawings are used as the basis for skeletal geometry, this aspect is the least susceptible to error, judging from the congruence between our measurements of *T. rex* AMNH 5027 and measurements scaled from Gregory Paul's drawings (Paul 1988). Accurate reconstructions of muscle topology are critical, but these can be derived rigorously using extant phylogenetic bracketing and extrapolatory inference (Bryant and Russell 1992; Witmer 1995).

The greatest potential for inaccuracy lies in reconstruction of individual muscle morphologies, cross-sectional areas, and other parameters of muscle function. Superficial muscles are unconstrained in how far they can be reconstructed to bulge away from the body, and their cross-sectional dimensions must be estimated through data available for extant relatives. Muscle pennation and other aspects of internal architecture can only be generally bracketed between extant sister taxa. Finally, superellipse area estimations are likely to underestimate cross-sectional areas for deep muscles that can fill in the entire space between superficial neighbors.

Limitations and Mitigating Factors of This Implementation of the Method

The current analysis of feeding dynamics in *T. rex* has several potential shortcomings. First, the muscle/tendon correlations of cross-sectional sizes rely on data from extant crocodilians and on extrapolation to *T. rex*. Nevertheless, the reconstructed dimensions of M. trans. cap. and M. long. cap. sup. on this specimen of *T. rex* appear reasonable in that they would not interfere with joint range of motion or the action of other muscles. Second, the reconstructed cross-sectional dimensions of M. complexus may be too large, as they are not constrained dorsoventrally. Third, the lines of pull of M. long. cap. sup., M. il. cap., and M. trans. cap. are undoubtedly unfavorably conservative. Most fascicles of these muscles in crocodilians do not take straight-line routes from origin to insertion, but rather take a path more orthogonal to each muscle's moment arm. However, the origins and insertions are physical data points, and choosing them as endpoints of tension vectors minimizes speculation and extrapolatory assumptions. The only exceptions were for M. transversospinalis capitis and M. transversospinalis cervicis in one lateroflexed posture, in which vertebrae blocked straight lines from origin to insertion.

Finally and most importantly, the insertion of M. complexus and origins of M. iliocostalis capitis in *T. rex* are ambiguous. We reconstruct M. complexus as inserting fully on the squamosals, which is reasonable considering a partial insertion here of the crocodilian homolog (Tsuihiji 2005), and insertions on the lateral occiput of many birds (including dissected *Aquila chrysaetos* and *Pelicanus occidentalis*). However, the muscle inserts primarily on the parietals in many birds, and its homolog in crocodilians, a lateral division of M. transver-

TABLE 8. Concentric accelerations and work generating capacity (isometric and eccentric ''accelerations'') of the feeding apparatus of *Tyrannosaurus rex* (AMNH 5027), imparted by M. longissimus capitis superficialis and profundus. Rotational inertias vary. Note that accelerations by M. longissimus capitis superficialis were highest when the head and neck were in a dorsiflexed (extended) posture.

	M. longissimus capitis superficialis				M. longissimus capitis profundus			
			Accelerations: rad/s^2				Accelerations: rad/s^2	
	Moments: N·m		I = 48.59	I = 280.19	Moments: N·m		I = 48.59	I = 48.59
	L-flex.	D-flex. (bilat.)	L-flex.	D-flex. (bilat.)	L-flex.	V-flex. (bilat.)	L-flex.	V-flex. (bilat.)
Neutral pose								
Concentric	1353.7	1299.6	27.9	4.6	191.9	383.8	3.9	7.9
Isometric	1692.2	1624.5	34.8	5.8	239.9	479.7	4.9	9.9
Eccentric low	2256.2	2166.0	46.4	7.7	319.8	639.6	6.6	13.2
Eccentric high	2707.4	2599.1	55.7	9.3	383.8	767.6	7.9	15.8
Dorsiflexed								
Concentric	1577.1	1350.0	32.5		168.8	337.7	3.5	6.9
Isometric	1971.3	1687.4	40.6		211.1	422.1	4.3	8.7
Eccentric low	2628.4	2249.9	54.1		281.4	562.8	5.8	11.6
Eccentric high	3154.1	2699.9	64.9		337.7	675.4	6.9	13.9
Ventroflexed								
Concentric	1469.1	1257.5	30.2		211.0	422.0	4.3	8.7
Isometric	1836.3	1571.9	37.8		263.7	527.5	5.4	10.9
Eccentric low	2448.4	2095.9	50.4		351.7	703.3	7.2	14.5
Eccentric high	2938.1	2515.0	60.5		422.0	844.0	8.7	17.4
Flexed right side								
Concentric	1208.8	1160.5	24.9		188.0	376.0	3.9	7.7
Isometric	1511.0	1450.6	31.1		235.0	469.9	4.8	9.7
Eccentric low	2014.7	1934.1	41.5		313.3	626.6	6.4	12.9
Eccentric high	2417.7	2321.0	49.8		376.0	751.9	7.7	15.5
Extended left side								
Concentric	1174.2	1127.2	24.2		206.4	412.7	4.2	8.5
Isometric	1467.7	1409.0	30.2		258.0	515.9	5.3	10.6
Eccentric low	1956.9	1878.7	40.3		343.9	687.9	7.1	14.2
Eccentric high	2348.3	2254.4	48.3		412.7	825.5	8.5	17.0

sospinalis capitis (Tsuihiji 2005), can encroach on the parietals at the insertion (Frey 1988). We interpret the single rugose scar on each parietal of *T. rex* as the sole insertion of M. transversospinalis capitis, but if part of M. complexus attached here the latter muscle's size and summation of pull would differ slightly from our estimates. The insertion of M. il. cap. along the ventral edge of the exoccipitals of *T. rex* is unambiguously bracketable, but its origins are not. If M. il. cap. did not originate from the proximal cervical ribs as proposed here (Fig. 1), but instead from fascia of anterior cervical ribs as in crocodilians, it would have a more medially directed pull and probably a smaller cross-section than our results indicate. We find a crocodilian-like origin of M. il. cap. unlikely in large theropods. Their rib shafts are much more gracile than the robust anterior ribs of crocodilians (especially in tyrannosaurids), and are closely appressed not only anteriorly but along the entire cervical column.

Despite these cautions, the capacity of *Tyrannosaurus rex* for inertial feeding is quite insensitive to reconstruction errors. Even with the complete absence of interspinous ligaments (analysis 1), dorsiflexive accelerations would diminish by only 15–16% (see results for Magnitude 1). Variation in antorbital density has a potentially greater effect (analysis 2), with rotational inertia of the head increasing by 20% if the antorbital space had a specific gravity of 1 versus that of air. This is highly unlikely given our understanding of pneumatization in *T. rex* and other archosaurs (Witmer 1997). Finally, bilateral moment-generating capacity of collective dorsiflexors and M. transversospinails

TABLE 9. Concentric accelerations and work generating capacity (isometric and eccentric ''accelerations'') of the feeding apparatus of *Tyrannosaurus rex* (AMNH 5027), imparted by M. iliocostalis capitis and M. rectus capitis ventralis. Rotational inertias are 48.59 kg·m^2. Note that M. rectus capitis ventralis was capable of more powerful ventroflexion than was M. longissimus capitis profundus (Table 8).

	M. iliocostalis capitis				M. rectus capitis ventralis			
	Moments: N·m		Accelerations: rad/s^2		Moments: N·m		Accelerations: rad/s^2	
	L-flex.	V-flex. (bilat.)	L-flex.	V-flex. (bilat.)	L-flex.	V-flex. (bilat.)	L-flex.	V-flex. (bilat.)
Neutral pose								
Concentric	602.8	456.2	12.4	9.4	232.8	640.2	4.8	13.2
Isometric	753.5	570.2	15.5	11.7	291.0	800.2	6.0	16.5
Eccentric low	1004.7	760.3	20.7	15.6	388.0	1067.0	8.0	22.0
Eccentric high	1205.6	912.3	24.8	18.8	465.6	1280.4	9.6	26.3
Dorsiflexed								
Concentric	553.9	419.2	11.4	8.6	218.8	601.6	4.5	12.4
Isometric	692.4	524.0	14.2	10.8	273.4	752.0	5.6	15.5
Eccentric low	923.2	698.6	19.0	14.4	364.6	1002.6	7.5	20.6
Eccentric high	1107.8	838.3	22.8	17.3	437.5	1203.1	9.0	24.8
Ventroflexed								
Concentric	558.7	422.8	11.5	8.7	240.3	660.8	4.9	13.6
Isometric	698.3	528.5	14.4	10.9	300.4	826.0	6.2	17.0
Eccentric low	931.1	704.6	19.2	14.5	400.5	1101.3	8.2	22.7
Eccentric high	1117.3	845.5	23.0	17.4	480.6	1321.6	9.9	27.2
Flexed right side								
Concentric	497.4	376.4	10.2	7.7	236.0	649.0	4.9	13.4
Isometric	621.7	470.5	12.8	9.7	295.0	811.3	6.1	16.7
Eccentric low	828.9	627.3	17.1	12.9	393.3	1081.7	8.1	22.3
Eccentric high	994.7	752.8	20.5	15.5	472.0	1298.0	9.7	26.7
Extended left side								
Concentric	365.2	276.4	7.5	5.7	232.4	639.0	4.8	13.2
Isometric	456.6	345.5	9.4	7.1	290.4	798.7	6.0	16.4
Eccentric low	608.7	460.7	12.5	9.5	387.3	1065.0	8.0	21.9
Eccentric high	730.5	552.8	15.0	11.4	464.7	1277.9	9.6	26.3

capitis would have to drop to less than 20% and 33% of their estimated values, respectively, before accelerations drop below the magnitude necessary for inertial feeding, or for reorienting food in the mouth prior to swallowing (analysis 3: Fig. 7). This assumes that the head would dorsiflex through no more than 45°; with greater excursions the food would reach adequately high tangential velocities at even smaller muscular moments. Further conservative assumptions for analysis 3 are that no soft tissues were supporting the head against gravity, and that powerful lateroflexors would not be involved in modulating the food's orientation.

Implications for Feeding in *Tyrannosaurus rex*: Muscle Moments and Accelerations

Adult *Tyrannosaurus rex* were among the largest terrestrial vertebrates, and scaling of locomotor muscle mass (Hutchinson 2004b) and rotational inertia (Carrier et al. 2001) indicate deliberate speeds commensurate with their size, albeit with higher agility than in other giant theropods (Snively and Russell 2002, 2003; Henderson and Snively 2003; Snively et al. 2004). However, despite high inertia of the feeding apparatus, calculated moments of neck muscles suggest powerful deployment of the jaws for feeding. These results hold under conservative estimates of muscle force parameters. Although we are skeptical of higher levels of force determined with the tendon safety factor (TSF) method, they are surprisingly in step with estimates of bite force (e.g., 90,000 N for bilateral firing of M. transversospinalis capitis, versus 77,000 to over 300,000 N of jaw muscle force applied at the teeth [Meers 2003; Therrien et al. 2005]).

Application of neck muscle force depended

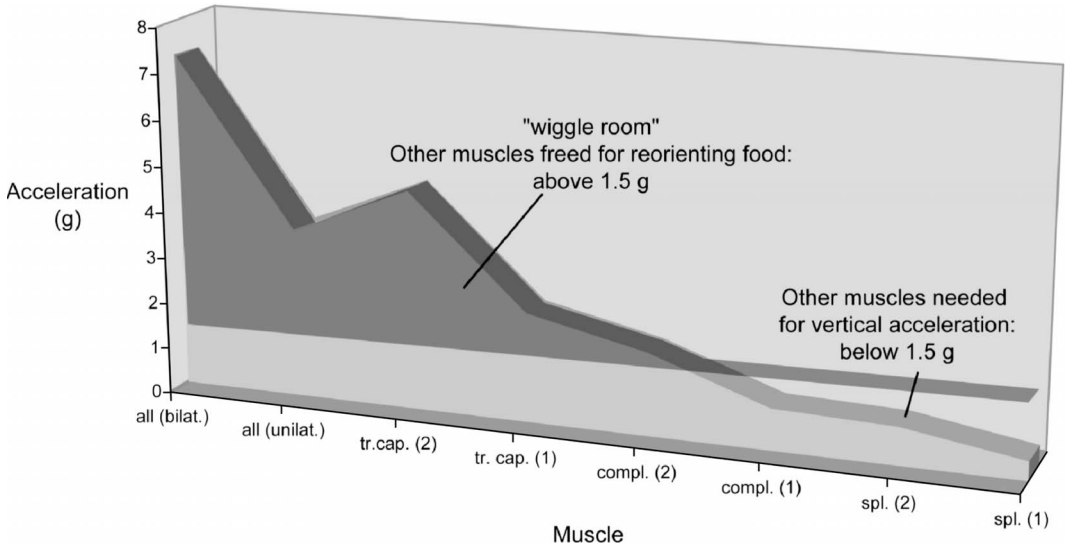

FIGURE 7. Sensitivity of inertial feeding in *Tyrannosaurus rex* to moment estimation error and muscle recruitment. Note that bilateral contraction by M. trans. cap. alone imparted over three times the acceleration necessary for inertial feeding under the specified conditions. The *x*-axis variables are combined, bilateral [bilat. or (2)] and individual unilateral [(unilat. or (1)] instances of muscle activation. The *y*-axis values are tangential accelerations in *g* ($\times$ 9.81 m/s^2) that muscles would impart to 490 N of food, 0.9 m from the occipital condyle. Acceleration values directly above single muscles or collective sets represent their maximum output. At 1.5 *g*, the food would be tossed high enough for inertial feeding. If a given muscle or set of muscles impart greater than 1.5 *g*, other muscles have recruitment latitude (''wiggle room'') for reorienting food in the mouth. Accelerations below 1.5 *g* impart insufficient tangential velocity to the food, necessitating additional muscle recruitment. Abbreviations: tr. cap., M. transversospinalis capitis. compl.; M. complexus. spl., M. splenius capitis; all, all of these three head dorsiflexors.

on orientation of the head and neck. Low variation in effective muscle pull with posture is consistent with the findings of Vasavada et al. (1998) for cat craniocervical muscles. Moment, acceleration, and work-generating capacities were lowest at extremes of lateral flexion, and highest when the head and neck were extended anteriorly in dorsiflexion. These findings suggest that adult *T. rex*, when tearing sideways, could perform the greatest work of fracture on food when the head was extended, but that for tearing sagittally it did not necessarily have a preferred posture (as is evident from the results yielded in testing Hypothesis 2). M. longissimus capitis superficialis was the most powerful lateroflexor in most postures, but its WGC diminished relative to M. complexus once the head and neck were fully lateroflexed. M. transversospinalis capitis had high WGC for dorsiflexion in all postures restricted to the midsagittal plane. WGC of M. transversospinalis cervicis was lower. However, the more posterior insertions of M. trans. cerv. (and concomitantly large distances [radii of rotation] to the head's center of mass) contributed to high tangential accelerations of the head.

Lateral and dorsiflexive accelerations of the head and neck were rapid in adult *Tyrannosaurus rex*, despite its great size. Gaze shifts for tracking prey, and strikes at prey as seen in birds (Snively 2006) and crocodilians, are therefore inferable as having been rapid as well. This indicates that *T. rex* was capable of striking prey rapidly without the need to secure it for an extended period with the diminished forelimbs. However, until accelerations of the feeding apparatus are assessed for large theropods with larger arms, we cannot conclude that *T. rex* compensated for reduced forelimbs with rapid strikes, or that it was more adept than large-armed carnosaurs at accelerating its head for attack.

Hypothesis 3, that adult *T. rex* could engage in inertial feeding with a 50-kg bolus of food, is strongly confirmed. At maximum dorsiflexive acceleration, a flick of the head would impart a final tangential velocity to the food of

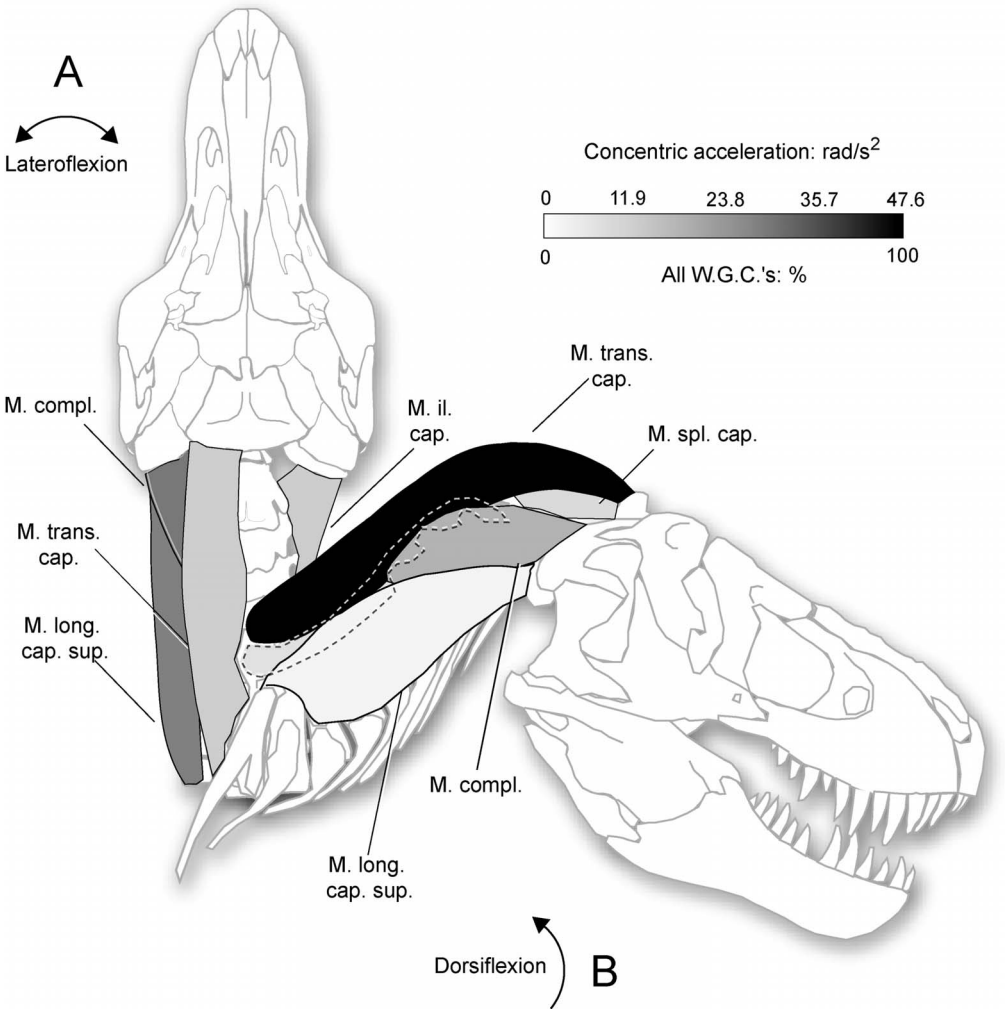

FIGURE 8. Summary of latero- and dorsiflexive capabilities (indicated by arrows) of major *T. rex* craniocervical muscles, with the head held in a neutral posture. Capacities are color coded, with black indicating the greatest absolute and relative values. Note that dorsiflexors could do more work than muscles acting collectively in lateroflexion (with capacity doubling under bilateral contraction), and that M. transversospinalis capitis imparted the highest radial accelerations. Abbreviations are as in Figure 2 and Table 2, except for M. complexus (M. compl.). A, Relative work-generating capacities (W.G.C.; percentages) and concentric accelerations (rad/s^2) of *T. rex* lateroflexive muscles, mapped onto a dorsal view of the skull and neck. M. complexus is partly outlined in white, for contrast with M. long. cap. sup. ventral to it. M. transversospinalis capitis was likely broader than depicted here. B, W.G.C. and concentric accelerations of major *T. rex* head dorsiflexors, mapped onto a lateral skeletal reconstruction. M. transversospinalis cervicis is deepest and depicted anteriorly with dashed outlines; posteriorly, it is color coded by its ability (relative to M. trans. cap.) to impart tangential acceleration to the rostrum.

nearly 10 m/s, which would send the food 5 m into the air if released. By using high muscle torques, *T. rex* could accelerate much greater masses of food adequately for inertial feeding. This maximal capacity undoubtedly was rarely used, and instead sets an upper bound on the spectrum of feeding abilities in adult *Tyrannosaurus rex*. Muscle accelerative capacity above the minimum threshold would exemplify momentarily excessive construction (Gans 1979), whereby reserve capabilities enable an animal to accomplish rare but selectively critical activities beyond its ordinary requirements. Sensitivity analysis 3 indicates that adult *T. rex* could easily toss food upwards for inertial feeding by submaximal sagittal accelerations, leaving muscle force available for lateral acceleration and reorientation

of food for swallowing. Accelerations of the feeding apparatus of *T. rex* were clearly adequate to mirror inertial feeding behavior observed in extant archosaurs, such as raptorial birds (Snively 2006) and crocodilians (Cleuren and De Vree 2000).

Implications of Interspinous Ligament Strengths

Calculated strengths appear to corroborate the hypothesis that ligaments maintained neck posture in *Tyrannosaurus rex* without the need for muscular effort. The extremely high safety factors are for static support only, and would diminish under heavy loads and accelerations. However, even with radically low collagen content parallel to the line of tension, it appears that static support by ligaments would have left the neck muscles of *Tyrannosaurus rex* free to exert all their force for manipulation of the head and food. This was presumably the case for other tyrannosaurids. Hengst (2004) found that interspinous ligaments of *Gorgosaurus libratus* (CMI 2001.89.1) and *T. rex* (FMNH PR2081) had safety factors comparable to those found for *T. rex* (AMNH 5027) in this study. Although *T. rex* could engage in inertial feeding whether interspinous ligaments were present or not, the ligaments augmented the ability of muscles to accelerate the feeding apparatus and increased the animal's ultimate musculoskeletal capabilities.

Conclusions

The use of the neck of *Tyrannosaurus rex* during feeding entailed a multiplicity of possible combinations of muscle actions, and the data presented here on muscle moment-generating capacity and accelerations can be applied to any hypothesis of neck action or function. High work-generating capacity of *T. rex* neck muscles suggests tearing and inertial feeding capacities similar to those of raptorial birds and crocodilians.

Constraining investigations on the basis of such behavior of living relatives renders the questions tractable and is rigorously productive as a ''reality check'' on feeding possibilities. Future investigations must extrapolate comparatively in the other direction, from feeding biomechanics and morphology of adult *Tyrannosaurus rex* to neck function of smaller tyrannosaurids and other large theropod dinosaurs.

Acknowledgments

This research was supported by Alberta Ingenuity and Jurassic Foundation funding to E.S., National Sciences and Engineering Research Council Discovery grants to A.P.R., and field assessments through University of Calgary Research Services on behalf of the Alberta Historical Resources Act. We thank D. Henderson for constructive criticism, for discussion, and for calculating rotational inertias; N. Longrich, T. Carr, and H. Knoll for advice on figures; and F. Snively for assessing the dynamics. M. Butcher and D. Syme provided valuable feedback on muscle force-generating parameters. J. Gardner, N. Larson, C. Mehling, C. Collins, M. Henderson, S. Williams, W. Simpson, and the technical staffs at their respective institutions facilitated access to fossils or casts necessary for specimen modeling. Comments by T. Holtz and an anonymous reviewer substantially improved the manuscript.

Literature Cited

Akima, H., S. Kuno, H. Takahashi, T. Fukunaga, and S. Katsuta. 2000. The use of magnetic resonance images to investigate the influence of recruitment on the relationship between torque and cross-sectional area in human muscle. European Journal of Applied Physiology 83:475–480.

Bakker, R. T. 1998 (2000). Brontosaur killers: Late Jurassic allosaurids as sabre-tooth cat.analogues. Gaia 15:145–158.

Bakker, R. T., M. Williams, and P. J. Currie. 1988. *Nanotyrannus*, a new genus of pygmy tyrannosaur, from the latest Cretaceous of Montana. Hunteria 1(5).

Bamman, M. W., B. R. Newcomer, D. Larson-Meyer, R. L. Weisner, and G. R. Hunter. 2000. Evaluation of the strength-size relation in vivo using various muscle size indices. Medicine and Science in Sports and Exercise 32:1307–1313.

Brechue, W. F., and T. Abe. 2002. The role of FFM accumulation and skeletal muscle architecture in powerlifting performance. European Journal of Applied Physiology 86:327–336.

Brochu, C. A. 2003. Osteology of *Tyrannosaurus rex*: insights from a nearly complete skeleton and high-resolution computed tomographic analysis of the cranium. Journal of Vertebrate Paleontology 24(Suppl. to No. 4):1–138.

Bryant, H. N., and A. P. Russell. 1992. The role of phylogenetic analysis in the inference of unpreserved attributes of extinct taxa. Philosophical Transactions of the Royal Society of London B 337:405–418.

Carpenter, K., and M. B. Smith. 2001. Forelimb osteology and biomechanics of *Tyrannosaurus*: Pp. 90–116 *in* D. H. Tanke and K. Carpenter, eds. Mesozoic vertebrate life. Indiana University Press, Bloomington.

Carrier, D. R., R. M. Walter, and D. V. Lee. 2001. Influence of ro-

tational inertia on turning performance of theropod dinosaurs: clues from humans with increased rotational inertia. Journal of Experimental Biology 204:391–3926.

Charig, A. J., and A. C. Milner. 1997. *Baryonyx walkeri*, a fish-eating dinosaur from the Wealden of Surrey. Bulletin of the British Museum of Natural History (Geology) 53:11–70.

Cheng, E. J., and S. H. Scott. 2000. Morphometry of *Macaca mulatta* forelimb. I. Shoulder and elbow muscles and segment inertial parameters. Journal of Morphology 245:206–224.

Cleuren, J., and F. De Vree. 2000. Feeding in crocodilians. Pp. 337–358 *in* K. Schwenk, ed. Feeding: form, function, and evolution in tetrapod vertebates. Academic Press, San Diego.

Cong, L.-Y., L.-H., Hou, X.-C., Wu, and J.-F. Hou. 1998. The gross anatomy of *Alligator sinensis* Fauvel. Science Press, Beijing.

Coombs, W. P., Jr. 1978. Theoretical aspects of cursorial adaptations in dinosaurs. Quarterly Review of Biology 53:393–418.

Delp, S. L., and J. P. Loan. 1995. A graphics-based software system to develop and analyze models of musculoskeletal structure. Computers in Biology and Medicine 25:21–34.

Erickson, G. M., S. D. Van Kirk, J. Su, M. E. Levenston, W. E. Caler, and D. R. Carter. 1996. Bite-force estimation for *Tyrannosaurus rex* from tooth-marked bones. Nature 382:706–708.

Frey, E. 1988. Anatomie des Korperstammes von *Alligator mississippiensis* Daudin. Stuttgarter Beitrage zur Naturkunde A 424:1–106.

Fukunaga, T., M. Miyatani, M. Kouzaki, Y. Kawakami, and H. Kanehisa. 2001. Muscle volume is a major determinant of joint torque in humans. Acta Physiologica Scandinavica 172:249–255.

Gans, C. 1979. Momentarily excessive construction as the basis for protoadaptation. Evolution 331:227–233.

Gillooly, J. S., A. P. Allen, and E. L. Charnov. 2006. Dinosaur fossils predict body temperatures. PLoS Biology 4:1467–1469.

Gordon, J. E. 1978. Structures: or, why things don't fall down. Plenum, New York.

Guyton, A. C., and J. E. Hall. 1996. Textbook of medical physiology, 9th ed. Saunders, Philadelphia.

Halliday, D., R. Resnick, and J. Walker. 1994. Fundamentals of physics, 4th ed. Wiley, New York.

Henderson, D. M. 1999. A mathematical and computational analysis of the biomechanics of walking theropod dinosaurs. Ph.D. thesis, University of Bristol, Bristol, U.K.

———. 2002. The eyes have it: the sizes, shapes, and orientations of theropod orbits as indicators of cranium strength and bite force. Journal of Vertebrate Paleontology 22:766–778.

Henderson, D. M., and E. Snively. 2003. *Tyrannosaurus* en pointe: allometry minimized rotational inertia of large carnivorous dinosaurs. Proceedings of the Royal Society of London B 271(Suppl. 3):S57–S60.

Hengst, R. A. 2004. Gravity and the *T. rex* backbone. Journal of Vertebrate Paleontology 24(Suppl. to No. 3):69A–70A.

Hildebrand, M., and G. Goslow. 2001. Analysis of vertebrate structure, 5th ed. Wiley, New York.

Holtz, T. R., Jr. 1994. The phylogenetic position of the Tyrannosauridae: implications for theropod systematics. Journal of Paleontology 68:1100–1117.

———. 1995. The arctometatarsalian pes, an unusual structure of Cretaceous Theropoda (Dinosauria: Saurischia). Journal of Vertebrate Paleontology 14:480–519.

———. 2002. Theropod predation: evidence and ecomorphology. *In* P. H. Kelly, M. Koweleski, and T. A. Hansen, eds. Predator-prey interactions in the fossil record. Topics in Geobiology 17:325–340. Kluwer Academic/Plenum, New York.

———. 2004. Tyrannosauroidea. Pp. 111–136 *in* D. B. Weishampel, P. Dodson, and H. Osmólska, eds. The Dinosauria, 2d ed. University of California Press, Berkeley.

Horstmann, T., F. Mayer, J. Maschmann, A. Niess, K. Roecker, and H.-H. Dickhuth. 2001. Metabolic reaction after concentric and eccentric endurance-exercise of the knee and ankle. Medicine and Science in Sports and Exercise 33:791–795.

Hutchinson, J. R. 2004a. Biomechanical modeling and sensitivity analysis of bipedal running ability. I. Extant taxa. Journal of Morphology 262:421–440.

———. 2004b. Biomechanical modeling and sensitivity analysis of bipedal running ability. II. Extinct taxa. Journal of Morphology 262:441–461.

Hutchinson, J. R., and M. Garcia. 2002. *Tyrannosaurus* was not a fast runner. Nature 415:1018–1021.

Johnston, I. A. 1985. Sustained force development: specializations and variation among the vertebrates. Journal of Experimental Biology 115:219–251.

Juul-Kristensen, B., F. Bojsen-Møller, L. Finsen, J. Eriksson, G. Johansson, F. Ståhlberg, and C. Ekdahl. 2000. Muscle sizes and moment arms determined by magnetic resonance imaging. Cells, Tissues, Organs 167:214–222.

Kawakami, Y., T. Abe, S. Y. Kun, and T. Fukunaga. 1995. Training-induced changes in muscle architecture and specific tension. European Journal of Applied Physiology 72:37–43.

Keshner, E. A., K. D. Statler, and S. L. Delp. 1997. Kinematics of the freely moving head and neck of the cat. Experimental Brain Research 115:257–266.

Lindstedt, S. L., P. C. LaStayo, and T. E. Reich. 2001. When active muscles lengthen: properties and consequences of eccentric contractions. News in Physiological Sciences 16:256–261.

Meers, M. B. 2003. Maximum bite force and prey size of *Tyrannosaurus rex* and their relationship to the inference of feeding behavior. Historical Biology 16:1–12.

Molnar, R. E. 1973. The cranial morphology of *Tyrannosaurus rex* (Reptilia: Saurischia). Ph.D. dissertation. University of California, Los Angeles.

———. 1998 (2000). Mechanical factors in the design of the cranium of *Tyrannosaurus rex* (Osborn 1905). Gaia 15:193–218.

Motani, R. 2001. Estimating body mass from silhouettes: testing the assumption of elliptical body cross-sections. Paleobiology 27:735–750.

Ng, B. H., S. M. Chou, B. H. Lim, and A. Chuong. 2004. Strain rate effect on the failure rate of tendons. Proceedings of the Institution of Mechanical Engineers, Part H, Journal of Engineering in Medicine 218:203–206.

Paul, G. S. 1988. Predatory dinosaurs of the world: a complete illustrated guide. Simon and Schuster, New York.

Pearsall, A. W., J. M. Hollis, G. V. Russell, and Z. Scheer. 2003. A biomechanical comparison of three lower extremity tendons for ligamentous reconstruction about the knee. Arthroscopy 19:1091–1096.

Provenzano, P. P., D. Heisey, K. Hayashi, R. Lakes, and R. Vanderby Jr. 2002. Subfailure damage in ligament: a structural and cellular evaluation. Journal of Applied Physiology 92: 362–371.

Rayfield, E. J. 2004. Cranial mechanics and feeding in *Tyrannosaurus rex*. Proceedings of the Royal Society of London B 271: 1451–1459.

———. 2005. Aspects of comparative cranial mechanics in the theropod dinosaurs. *Coelophysis*, *Allosaurus* and *Tyrannosaurus*. Zoological Journal of the Linnean Society 144:309–316.

Rayfield, E. J., D. B. Norman, C. C. Horner, J. R. Horner, P. May Smith, J. J. Thomason, and P. Upchurch. 2001. Cranial design and function in a large theropod dinosaur. Nature 409:1033–1037.

Richmond, F. J. R. 1998. Elements of style in neuromuscular architecture. American Zoologist 38:729–742.

Rosse, C., and P. Gaddum-Rosse. 1997. Hollinshead's textbook of anatomy, 5th ed. Lippincott-Raven, Philadelphia.

Schechtman, H., and D. L. Bader. 2002. Fatigue damage of human tendons. Journal of Biomechanics 35:347–353.

Seidel, R. 1978. The somatic musculature of the cervical and oc-

cipital regions of *Alligator mississippiensis*. Ph.D. dissertation. City University of New York, New York.

Selbie, W. S., D. B. Thomson, and F. J. R. Richmond. 1993. Sagittal-plane mobility of the cat cervical spine. Journal of Biomechanics 26:917–927.

Senter, P., and J. H. Robins. 2005. Range of motion in the forelimb of the theropod dinosaur *Acrocanthosaurus atokensis*, and implications for predatory behavior. Journal of Zoology 266: 307–318.

Snively, E. 2006. Neck musculoskeletal function in the Tyrannosauridae (Theropoda, Coelurosauria): implications for feeding dynamics. Ph.D. thesis, University of Calgary, Calgary, Alberta.

Snively, E., and A. P. Russell. 2002. The tyrannosaurid metatarsus: bone strain and inferred ligament function. Senckenbergiana Lethaea 82:35–42.

———. 2003. A kinematic model of tyrannosaurid (Dinosauria, Theropoda) arctometatarsus function. Journal of Morphology 255:215–227.

Snively, E., A. P. Russell, and G. L. Powell. 2004. Evolutionary morphology of the coelurosaurian arctometatarsus: descriptive, morphometric, and phylogenetic approaches. Zoological Journal of the Linnean Society 142:525–553.

Snively, E., D. M. Henderson, and D. S. Phillips. 2006. Fused and vaulted nasals of tyrannosaurid dinosaurs: implications for cranial strength and feeding mechanics. Acta Palaeontologica Polonica 51:435–454.

Stevens, K. A., and M. J. Parrish. 1999. Neck posture in two Jurassic sauropod dinosaurs. Science 284:798–800.

Syme, D. A. 2006. Functional properties of skeletal muscle. Fish Biomechanics 23:179–240.

Therrien, F., D. M. Henderson, and C. B. Ruff. 2005. Bite me: biomechanical models of theropod mandibles and implications for feeding behavior. Pp. 179–237 *in* K. Carpenter, ed. The carnivorous dinosaurs. Indiana University Press, Bloomington.

Thorpe, S. K. S., R. H. Crompton, M. M. Günther, R. F. Ker, and R. M. Alexander. 1999. Dimensions and moment arms of the hind- and forelimb muscles of common chimpanzees. American Journal of Physical Anthropology 110:179–199.

Tsuihiji, T. 2005. Homologies of the transversospinalis muscles in the anterior presacral region of Sauria (crown Diapsida). Journal of Morphology 263:151–178.

Vasavada, A. N., S. Li, and S. L. Delp. 1998. Influence of muscle morphometry and moment arms on the moment-generating capacity of human neck muscles. Spine 23:412–422.

Wedel, M. J. 2004. Skeletal pneumaticity in saurischian dinosaurs and its implications for mass estimates. Journal of Vertebrate Paleontology 24(Suppl. to No. 3):127A.

Wegweiser, M. B., B. Breithaupt, and R. Chapman. 2004. Attack behavior of tyrannosaurid dinosaur(s): Cretaceous crime scenes, really old evidence, and ''smoking guns.'' Journal of Vertebrate Paleontology 24(Suppl. to No. 3):127A.

Witmer, L. M. 1995. The extant phylogenetic bracket and the importance of reconstructing soft tissues in fossils. Pp. 19–33 *in* J. J. Thomason, ed. Functional morphology in vertebrate paleontology. Cambridge University Press, Cambridge.

———. 1997. The evolution of the antorbital cavity of archosaurs: a study in soft tissue reconstruction in the fossil record with an analysis of the function of pneumaticity. Society of Vertebrate Paleontology Memoir 3. Journal of Vertebrate Paleontology 17 (Suppl. to No. 1).

Wroe, S., C. McHenry, and J. Thomason. 2005. Bite club: comparative bite force in big biting mammals and the prediction of predatory behavior in fossil taxa. Proceedings of the Royal Society of London B 272:619–625.

Yamaguchi, G. T. 2001. Dynamic modeling of the musculoskeletal system: a vectorized approach for biomechanical analysis in three dimensions. Kluwer Academic, Boston.